ALS and PD (Ishigaki et al., 2004). Moreover, formation of this complex was found to be necessary for the E3 activity of Dorfin against mutant SOD1. These findings suggest that Dorfin is involved in the quality-control system for the abnormal proteins that accumulate in the affected neurons in neurodegenerative disorders.

Dorfin degrades mutant SOD1s and attenuates mutant SOD1-associated toxicity in cultured cells (Niwa et al., 2002). However, in Dorfin/mutant SOD1 double transgenic mice, we found only a modest beneficial effect on mutant SOD1-induced survival and motor dysfunction (unpublished data). These findings, combined with the short half-life of Dorfin protein, led us to hypothesize that the limiting effect of the Dorfin transgene may be a consequence of autodegradation of Dorfin, since Dorfin can execute autoubiquitilation *in vivo* (Niwa et al., 2001).

Carboxyl terminus of Hsc70-interacting protein (CHIP) is also an E3 protein; it has a TPR domain in the N terminus and a U-box domain in the C terminus. The U-box domain of CHIP is responsible for its strong E3 activity, whereas the TPR domain recruits heat shock proteins harboring misfolded client proteins such as cystic fibrosis transmembrane conductance regulator (CFTR), denatured luciferase, and tau (Meacham et al., 2001; Murata et al., 2001, 2003; Hatakeyama et al., 2004; Shimura et al., 2004).

To prolong the protein lifetime of Dorfin and thereby obtain more potent ubiquitylation and degradation activity against mutant SOD1s than is provided by Dorfin or CHIP alone, we generated chimeric proteins containing the substrate-binding domain of Dorfin and the UPR domain of CHIP substitute for RING/IBR of Dorfin. We developed 12 candidate constructs that encode Dorfin-CHIP chimeric proteins and analyzed them for their E3 activities and degradation abilities against mutant SOD1 protein in cultured cells.

Experimental procedures

Plasmids and antibodies

We designed constructs expressing Dorfin-CHIP chimeric protein. In these constructs, different-length fragments of the C-terminus portion of Dorfin, including the hydrophobic substrate-binding domain (amino acids 333–838, 333–700, and 333–454) and the C-terminus UPR domain of CHIP with amino acids 128–303 or without amino acids 201–303, a charged region was fused in various combinations as shown in Fig. 2C. Briefly, Dorfin-CHIP$^{A, B, C, G, H,}$ and ^{I} had the C-terminus portion of Dorfin in their N-terminus and the U-box of CHIP in their C-terminus; Dorfin-CHIP$^{D, E, F, J, K}$, and ^{L} had the U-box of CHIP in their N-terminus and the C-terminus portion of Dorfin in their C-terminus.

We prepared a pCMV2/FLAG-Dorfin-CHIP chimeric vector (Dorfin-CHIP) by polymerase chain reaction (PCR) using the appropriate design of PCR primers with restriction sites (*Cla*I, *Kpn*I, and *XBa*I or *Eco*RI, *Cla*I, and *Kpn*I). The PCR products were digested and inserted into the *Cla*I–*Kpn*I site in pCMV2 vector (Sigma, St. Louis, MO). These vectors have been described previously: pFLAG-Dorfin^{WT} (Dorfin^{WT}), FLAG-Dorfin$^{C132S/C135S}$ (Dorfin$^{C132S/C135S}$), pFLAG-CHIP (CHIP), pFLAG-Mock (Mock), pcDNA3.1/Myc-SOD1^{WT} (SOD1^{WT}), pcDNA3.1/Myc-SOD1^{G93A} (SOD1^{G93A}), pcDNA3.1/Myc-SOD1^{G85R} (SOD1^{G85R}), pcDNA3.1/Myc-SOD1^{H46R} (SOD1^{H46R}), pcDNA3.1/Myc-SOD1^{G37R} (SOD1^{G37R}), pEGFP/SOD1^{WT} (SOD1^{WT}-GFP), and pEGFP/SOD1^{G85R} (SOD1^{G85R}-GFP) (Ishigaki et al., 2004). We used monoclonal anti-FLAG antibody (M2; Sigma), monoclonal anti-Myc antibody (9E10; Santa Cruz Biotechnology, Santa Cruz, CA), monoclonal anti-HA antibody (12CA5; Roche, Basel, Switzerland), and polyclonal anti-SOD1 (SOD-100; Stressgen, San Diego, CA).

Cell culture and transfection

We grew HEK293 cells and neuro2a (N2a) cells in Dulbecco's modified Eagle's medium (DMEM) containing 10% fetal calf serum (FCS), 5 U/ml penicillin, and 50 μg/ml streptomycin. At subconfluence, we transfected these cells with the indicated plasmids, using Effectene reagent (Qiagen, Valencia, CA) for HEK293 cells and Lipofectamine 2000 (Invitrogen, Carlsbad, CA) for N2a cells. After overnight posttransfection, we treated the cells with 1 μM MG132 (Z-Leu-Leu-Leu-al; Sigma) for 16 h to inhibit cellular proteasome activity. We analyzed the cells 24–48 h after transfection. To differentiate N2a cells, cells were treated for 48 h with 15 μM of retinoic acid in 2% serum medium.

Immunological analysis

At 24–48 h after transfection, we lysed cells (4×10^5 in 6-cm dishes) with 500 μl of lysis buffer consisting of 50 mM Tris–HCl, 150 mM NaCl, 1% Nonidet P-40, and 1 mM ethylenediaminetetraacetic acid (EDTA), as well as a protease inhibitor cocktail (Complete Mini, Roche). The lysate was then centrifuged at $10{,}000\times g$ for 10 min at 4°C to remove debris. We used a 10% volume of the supernatants as the lysate for SDS-PAGE. When immunoprecipitated, the supernatants were precleared with protein A/G agarose (Santa-Cruz). A specific antibody, either anti-FLAG (M2) or anti-Myc (9E10), was then added. We incubated the immune complexes, first at 4°C with rotation and with protein A/G agarose (Roche) for 3 h, after which they were collected by centrifugation and washed four times with the lysis buffer. For protein analysis, immune complexes were dissociated by heating in SDS-PAGE sample buffer and loaded onto SDS-PAGE. We separated the samples by SDS-PAGE (15% gel or 5%–20% gradient gel) and transferred them onto polyvinylidene difluoride membranes. We then immunoblotted samples with specific antibodies.

Immunohistochemistry

We fixed differentiated N2a cells grown in plastic dishes in 4% paraformaldehyde in PBS for 15 min. The cells were then blocked for 30 min with 5% (vol/vol) normal goat serum in PBS, incubated overnight at 4°C with anti-FLAG antibody (M2), washed with PBS, and incubated for 30 min with Alexa 496 nm anti-mouse antibodies (Molecular Probes, Eugene, OR). We mounted the cells on slides and obtained images using a fluorescence microscope (IX71; Olympus, Tokyo, Japan) equipped with a cooled charge-coupled device camera (DP70; Olympus). Photographs were taken using DP Controller software (Olympus).

Analysis of protein stability

We assayed the stability of proteins by pulse-chase analysis using [^{35}S] followed by immunoprecipitation. Metabolic labeling was performed as described previously (Yoshida et al., 2003). Briefly, in the pulse-chase analysis of Dorfin proteins, HEK293 cells in 6-cm dishes were transiently transfected with 1 μg of

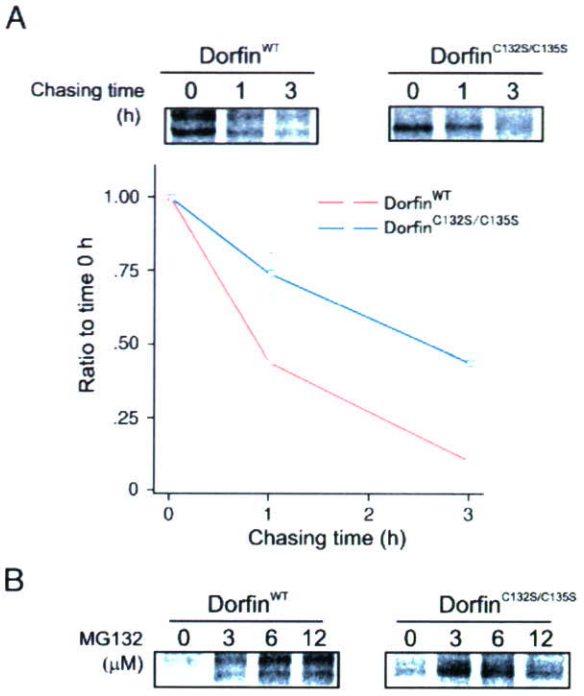

Fig. 1. Pulse-chase analysis of Dorfin^{WT} and Dorfin$^{C132S/C135S}$. (A) Dorfin^{WT} or Dorfin$^{C132S/C135S}$ was overexpressed in HEK293 cells. After overnight incubation, [^{35}S]-labeled Met/Cys pulse-chase analysis was performed. Cells were harvested and analyzed at 0, 1, or 3 h after labeling and immunoprecipitation by anti-FLAG antibody (upper panels). To determine serial changes in the amount of Dorfin^{WT} or Dorfin$^{C132S/C135S}$, four independent experiments were performed and the amounts of Dorfin^{WT} and Dorfin$^{C132S/C135S}$ were plotted. The differences between the amounts of Dorfin^{WT} and Dorfin$^{C132S/C135S}$ were significant at 1 h ($p<0.01$) and 3 h after labeling ($p<0.001$) (lower panels). Values are the means±SE, $n=4$. Statistics were done using an unpaired t-test. (B) Cells overexpressing Dorfin^{WT} or Dorfin$^{C132S/C135S}$ were treated with different concentrations of MG132 for 3 h after labeling.

FLAG-Dorfin^{WT} or FLAG-Dorfin$^{C132S/C135S}$. In pulse-chase experiments using SOD1^{G85R}, N2a cells in 6-cm dishes were transiently transfected with 1 μg of SOD1^{G85R}-Myc or SOD1^{G93A}-Myc and FLAG-Mock, FLAG-Dorfin, or FLAG-Dorfin-CHIP^{L}. FLAG-Mock was used as a negative control. After starving the cells for 60 min in methionine- and cysteine-free DMEM with 10% FCS, we labeled them for 60 min with 150 μCi/ml of Pro-Mix L-[^{35}S] *in vitro* cell-labeling mix (Amersham Biosciences). Cells were chased for different lengths of time at 37°C. In experiments with proteasomal inhibition, we added different amounts of MG132 in medium during the chase period. We performed immunoprecipitation using protein A/G agarose, mouse monoclonal anti-FLAG (M2), and anti-Myc (9E10). The intensity of the bands was quantified by ImageGauge software (Fuji Film, Tokyo, Japan).

MTS assay

We transfected N2a cells (5000 cells per well) in 96-well collagen-coated plates with 0.15 μg of SOD1^{G85R}-GFP and 0.05 μg of Dorfin, CHIP, Dorfin-CHIP^{L}, or pCMV2 vector (Mock) using Effecten reagent (Qiagen). Then we performed 3-(4,5-dimethylthiazol-2-yl)-5-(3-carboxymethoxyphenyl)-2-(4-sulfophenyl)-2*H*-tetrazolium inner salt (MTS) assays using Cell Titer 96 (Promega) at 48 h after incubation. This procedure has previously been described (Ishigaki et al., 2002a).

Aggregation assay

We transfected N2a cells in 6-cm dishes with 1.0 μg of SOD1^{G85R}-GFP and 1.0 μg of FLAG-Mock, FLAG-Dorfin, FLAG-CHIP, or FLAG-Dorfin-CHIP^{L}. After overnight incubation, we changed the medium to 2% FCS containing medium with 15 μM retinoic acid (RA) for differentiation. In the MG132 (+) group, 1 μM of MG132 was added after 24 h of differentiation stimuli. After 48 h of differentiation stimuli, we examined the cells in their living condition by fluorescence microscopy. The transfection ratio was equivalent (75%) among all groups. Visually observable macro aggregation-harboring cells were counted as "aggregation positive" cells (Fig. 7C). All cells were counted in fields selected at random from the four different quadrants of the culture dish. Counting was done by an investigator who was blind to the experimental condition.

Results

Dorfin degradation by the UPS in vivo

We analyzed the degradation speed of FLAG-Dorfin by the pulse-chase method using [^{35}S] labeling, finding that more than half of wild-type Dorfin (Dorfin^{WT}) was degraded within 1 h (Fig. 1A). This degradation was dose-dependently inhibited by MG132, a proteasome inhibitor (Fig. 1B). On the other hand, the RING mutant form of Dorfin (Dorfin$^{C132S/C135S}$), which lacks E3 activity (Ishigaki et al., 2004), degraded significantly more slowly than did Dorfin^{WT} (Fig. 1A and Table 1). As shown in Fig. 1A, Dorfin^{WT} showed two bands, whereas Dorfin$^{C132S/C135S}$ had a single band. This was also seen in our previous study (Ishigaki et al., 2004) and may represent posttranslational modification.

Construction of Dorfin-CHIP chimeric proteins

It is known that the C-terminus portion of Dorfin can bind to substrates such as mutant SOD1 proteins or Synphilin-1 (Niwa et al., 2002; Ito et al., 2003). We attempted to identify the domain of Dorfin that interacts with substrates. Although there was no obvious known motif in the C-terminus of Dorfin (amino acids 333–838), its first quarter contained rich hydrophobic amino acids (amino acids 333–454) (Fig. 2A). Immunoprecipitation analysis revealed that the hydrophobic region of Dorfin (amino acids 333–454) was able to bind to SOD1^{G85R}, indicating that this hydrophobic region is responsible for recruiting mutant SOD1 in Dorfin protein (Fig. 2B).

To establish more effective and more stable E3 ubiquitin ligase molecules that can recognize and degrade mutant SOD1s, we

Table 1
Serial changes in the amounts of Dorfin^{WT}, Dorfin$^{C132S/C135S}$, and Dorfin-CHIP^{L}

	0 h (%)	1 h (%)	3 h (%)
Dorfin^{WT}	100	43.7±7.0	10.3±4.4
Dorfin$^{C132S/C135S}$	100	73.9±13.8	43.7±1.9
Dorfin-CHIP^{L}	100	89.0±5.7	47.5±5.3

Values are the mean and SD of four independent experiments.

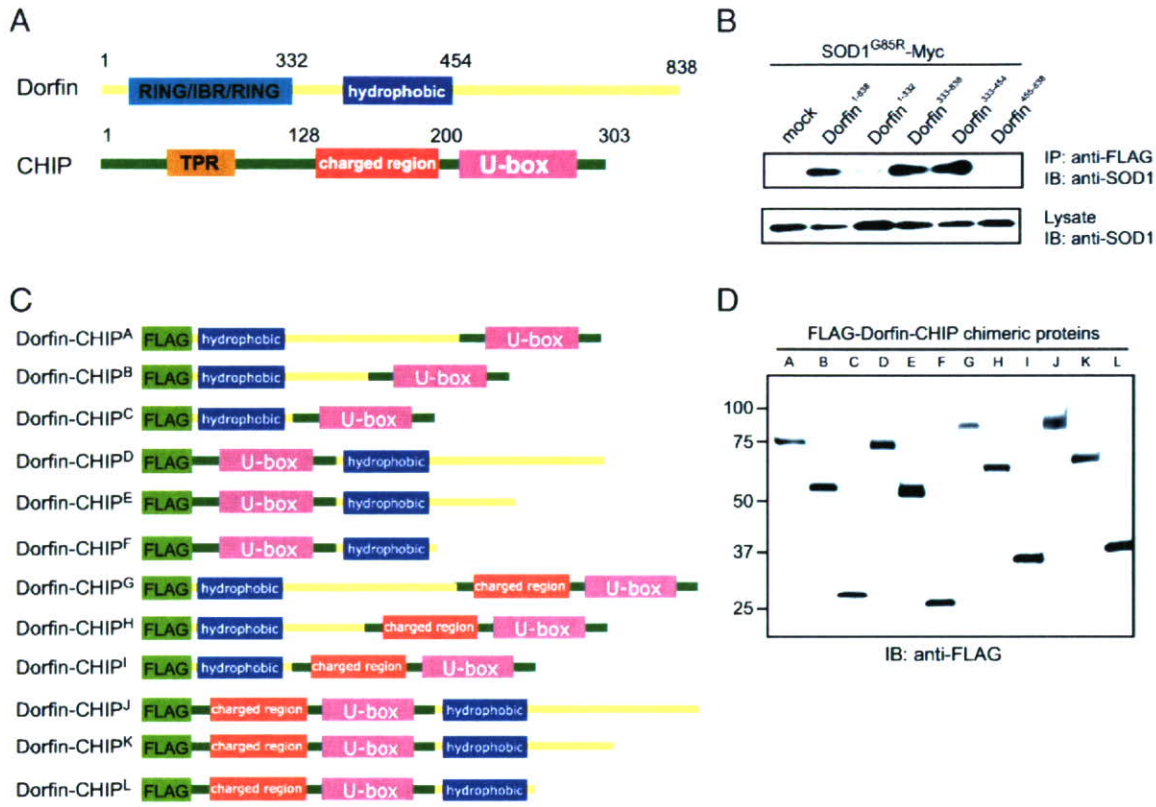

Fig. 2. Construction of Dorfin-CHIP chimeric proteins. (A) Dorfin has a RING/IBR domain in its N-terminus and a substrate-binding portion in the C-terminus. CHIP contains a TPR domain that binds to heat-shock proteins at the N-terminus; its C-terminal U-box domain has strong E3 ubiquitin ligase activity. (B) SOD1^{G85R}-Myc and FLAG-Dorfin derivatives were overexpressed in HEK 293 cells. Cell lysates were immunoprecipitated with anti-myc antibody. Immunoblotting showed that FLAG-Dorfin derivatives containing Dorfin$^{333-454}$ bound to SOD1^{G85R}-Myc, indicating that the hydrophobic region of Dorfin (Dorfin$^{333-454}$) is essential for interaction with mutant SOD1 *in vivo*. (C) Scheme of engineered Dorfin-CHIP chimeric proteins. Three different lengths of C-terminal Dorfin containing the hydrophobic region of Dorfin (Dorfin$^{333-454}$) and the U-box domain of CHIP with or without the charged region were fused. (D) Dorfin-CHIP chimeric proteins were overexpressed in HEK293 cells. Harvested cells were lysed and analyzed by immunoblotting using anti-FLAG antibody.

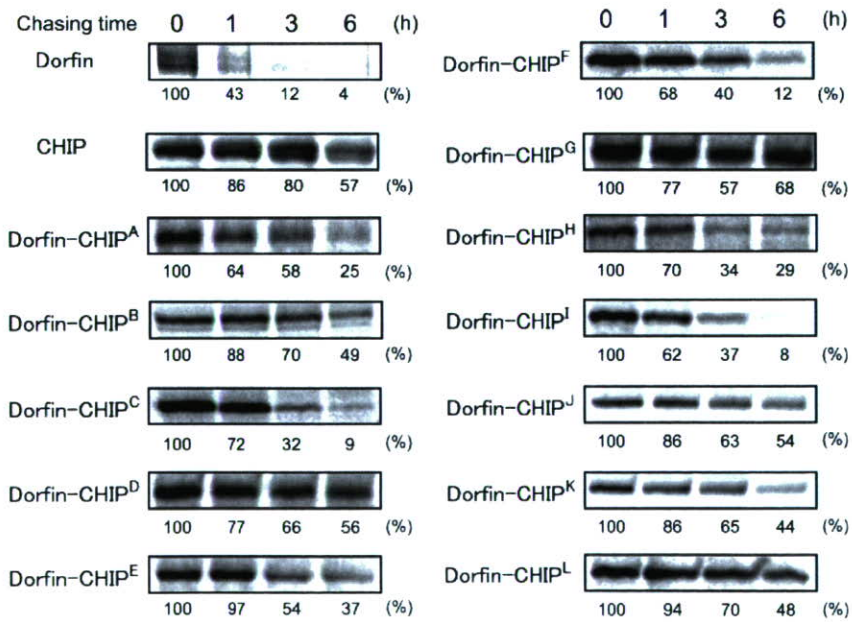

Fig. 3. The stability of Dorfin-CHIP chimeric proteins. Pulse-chase analysis using [^{35}S]-Met/Cys was performed. Dorfin, CHIP, and all the Dorfin-CHIP chimeric proteins were overexpressed in HEK293 cells and labeled with [^{35}S]-Met/Cys. Immunoprecipitation using anti-FLAG antibody and SOD-PAGE analysis revealed the degradation speed of FLAG-Dorfin-CHIP chimeric proteins. The amount of each Dorfin-CHIP chimeric protein was measured by quantifying the band using ImageGauge software.

designed Dorfin-CHIP chimeric proteins containing both the hydrophobic substrate-binding domain of Dorfin and the U-box domain of CHIP, which has strong E3 activity (Fig. 2C). We verified that all of the 12 candidate chimeric proteins were expressed in HEK293 cells (Fig. 2D).

Expression of Dorfin-CHIP chimeric proteins in cells

The half lives of all the Dorfin-CHIP chimeric proteins were more than 1 h. In some of these proteins, such as Dorfin-CHIP$^{D, G, J}$, and ^{L}, moderate amounts of protein still remained at 6 h after labeling, indicating that they were degraded much more slowly than was Dorfin^{WT} (Fig. 3). Repetitive experiments using Dorfin-CHIP^{L} yielded a significant difference between the amount of Dorfin^{WT} and Dorfin-CHIP^{L} at 1 h and 3 h (Table 1).

E3 activity of Dorfin-CHIP chimeric proteins against mutant SOD1

Immunoprecipitation analysis demonstrated that Dorfin and CHIP bound to mutant SOD1^{G85R} in equivalent amounts and that all of the Dorfin-CHIP chimeric proteins interacted with mutant SOD1^{G85R} *in vivo*. Dorfin-CHIP$^{A, D, E, F, J, K}$, and ^{L} bound to the same or greater amounts of SOD1^{G85R} than did Dorfin, whereas Dorfin-CHIP$^{B, C, G, H}$, and ^{I} did not (Fig. 4A, upper panel). None of the Dorfin-CHIP chimeric proteins bound to SOD1^{WT} *in vivo*

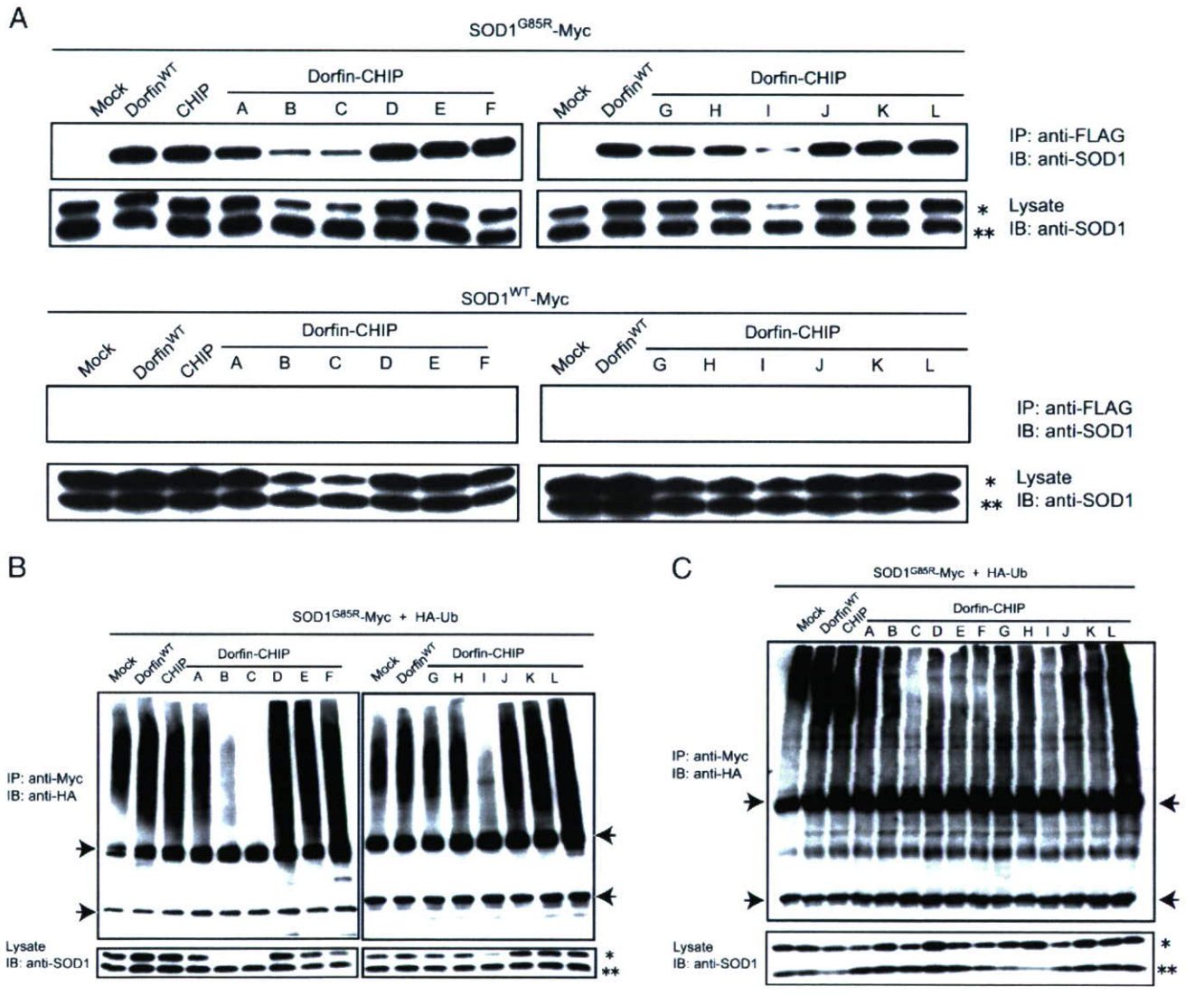

Fig. 4. The E3 activity of Dorfin-CHIP chimeric proteins on mutant SOD1 *in vivo*. (A) *In vivo* binding assay with both wild-type and mutant SOD1s. SOD1^{G85R}- or SOD1^{WT}-Myc and FLAG derivatives of Dorfin-CHIP chimeric proteins were coexpressed in HEK293 cells. Immunoprecipitation was done using anti-Myc antibody. Immunoblotting with anti-FLAG antibody revealed that all the Dorfin-CHIP chimeric proteins bound *in vivo* to SOD1^{G85R}-Myc but not to SOD1^{WT}-Myc. Single and double asterisks indicate overexpressed human SOD1s and mouse endogenous SOD1, respectively. (B) *In vivo* ubiquitylation assay in HEK293 cells. SOD1^{G85R}-Myc, HA-Ub, and FLAG derivatives of Dorfin-CHIP chimeric proteins were coexpressed in HEK293 cells. Immunoblotting with anti-HA antibody demonstrated the ubiquitylation level of SOD1^{G85R}-Myc by FLAG derivatives of Dorfin-CHIP chimeric proteins *in vivo*. Arrows indicate IgG light and heavy chains. Single and double asterisks indicate overexpressed SOD1 and mouse endogenous SOD1, respectively. (C) *In vivo* ubiquitylation assay in N2a cells. SOD1^{G85R}-Myc, HA-Ub, and FLAG derivatives of Dorfin-CHIP chimeric proteins were coexpressed in N2a cells. Arrows indicate IgG light and heavy chains. Single and double asterisks indicate overexpressed human SOD1s and mouse endogenous SOD1, respectively.

(Fig. 4A, lower panel). Some Dorfin-CHIP chimeric proteins, such as Dorfin-CHIP$^{B, C}$, and ^{I}, had lower amounts of both SOD1^{WT} and SOD1^{G85R} in the lysates. We performed quantitative RT-PCR using specific primers for SOD1-Myc, finding that coexpression of Dorfin-CHIP$^{B, C,}$ or ^{I} suppressed the mRNA expression of overexpressed SOD1 gene (Supplementary Fig. 1). Considering the possibility that these Dorfin-CHIP chimeric proteins might have unpredicted toxicity for cells by affecting gene transcription via unknown mechanisms, we excluded them from further analysis. Other Dorfin-CHIP proteins did not affect SOD1-Myc gene expression, which validated the comparison among IPs and ubiquitylated mutant SOD1 in Figs. 4A–C.

To assess the effectiveness of the E3 activity of Dorfin-CHIP chimeric proteins, we did an *in-vivo* ubiquitylation analysis by coexpression of SOD1^{G85R}-Myc, HA-Ub, and Dorfin-CHIP chimeric proteins in HEK293 cells. We found that Dorfin and CHIP enhanced the ubiquitylation of SOD1^{G85R} protein and that the ubiquitylation levels of these two E3 ligases were almost equivalent. Moreover, Dorfin-CHIP$^{D, E, F, J, K}$, and ^{L} ubiquitylated SOD1^{G85R} more effectively than did Dorfin or CHIP (Fig. 4B).

Performing the same *in-vivo* ubiquitylation assay using N2a cells, we observed that the levels of ubiquitylation of SOD1^{G85R} by Dorfin and CHIP were equivalent, as they were in HEK293 cells. Among Dorfin-CHIP chimeric proteins, only Dorfin-CHIP^{L}

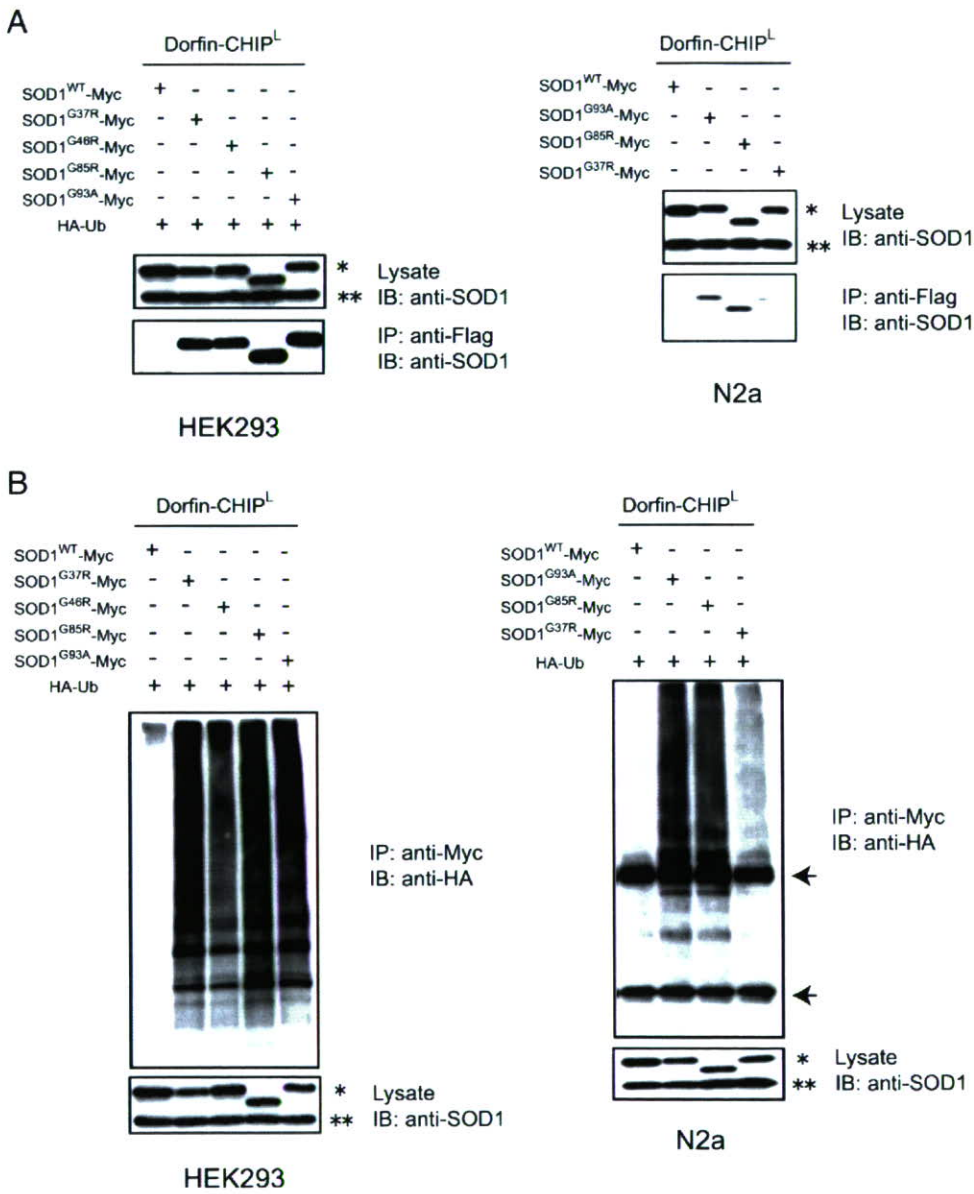

Fig. 5. Dorfin-CHIP^{L} specifically ubiquitylates mutant SOD1s *in vivo*. (A) *In vivo* binding assay with various mutant SOD1s. SOD1^{WT}-Myc, SOD1^{G93A}-Myc, SOD1^{G85R}-Myc, SOD1^{H46R}-Myc or SOD1^{G37R}-Myc, and FLAG-Dorfin-CHIP^{L} were coexpressed in HEK293 (left) and N2a cells (right). Immunoprecipitation was done using anti-Myc antibody. Immunoblotting with anti-FLAG antibody showed that both chimeric proteins specifically bound to mutant SOD1s *in vivo*. Single and double asterisks indicate overexpressed SOD1 and mouse endogenous SOD1, respectively. (B) *In vivo* ubiquitylation assay. SOD1^{WT}-Myc, SOD1^{G93A}-Myc, SOD1^{G85R}-Myc, SOD1^{H46R}-Myc or SOD1^{G37R}-Myc, as well as FLAG-Dorfin-CHIP^{L} and HA-Ub, was coexpressed in HEK293 (left) and N2a cells (right). Immunoblotting with anti-HA antibody showed the specific ubiquitylation of mutant SOD1-Myc by FLAG-Dorfin-CHIP^{L} *in vivo*. Arrows indicate IgG light and heavy chains. Single and double asterisks indicate overexpressed human SOD1s and mouse endogenous SOD1, respectively.

ubiquitylated SOD1^{G85R} more effectively than did Dorfin or CHIP, while Dorfin-CHIP$^{D, E, F, J}$, and ^{K} did not (Fig. 4C). Thus, Dorfin-CHIP^{L} was the most potent candidate of the chimeric proteins.

Ubiquitylation of mutant SOD1 by Dorfin-CHIP^{L}

Dorfin specifically ubiquitylated mutant SOD1 proteins, but not SOD1^{WT} protein (Niwa et al., 2002; Ishigaki et al., 2004). Similarly, Dorfin-CHIP^{L} interacted with SOD1^{G93A}, SOD1^{G85R}, SOD1^{H46R}, and SOD1^{G37R}, but not SOD1^{WT}, in HEK293 cells. This was confirmed in N2a cells (Fig. 5A). In both HEK293 and N2a cells, Dorfin-CHIP^{L} also ubiquitylated mutant SOD1 proteins but not SOD1^{WT} (Fig. 5B).

Degradation of mutant SOD1 by Dorfin-CHIP chimeric proteins

To assess the degradation activity of Dorfin-CHIP^{L} against mutant SOD1s, we performed the pulse-chase analysis on N2a

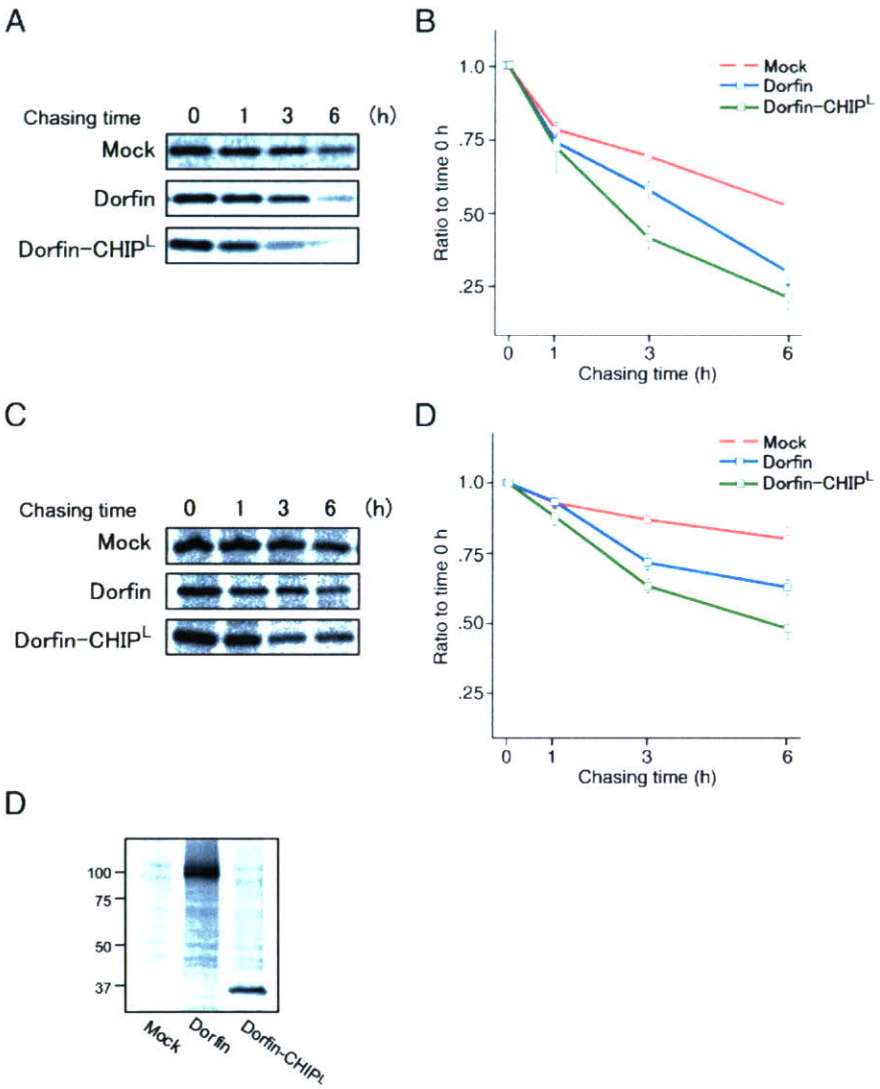

Fig. 6. Degradation of mutant SOD1 proteins with Dorfin-CHIP^{L}. (A) Pulse-chase analysis of SOD1^{G85R} with Dorfin-CHIP^{L}. N2a cells were coexpressed with SOD1^{G85R}-Myc and Mock, Dorfin, and Dorfin-CHIP^{L}. Pulse-chase experiments using [^{35}S]-Met/Cys were done. Immunoprecipitation using anti-Myc antibody and SOD-PAGE analysis revealed the degradation speed of SOD1^{G85R}-Myc. (B) Serial changes in the amount of SOD1^{G85R} coexpressed with Mock, Dorfin, or Dorfin-CHIP^{L}. Four independent experiments were performed and the amounts of SOD1^{G85R} were plotted. There were significant differences between Mock and Dorfin ($p<0.005$), Mock and Dorfin-CHIP^{L} ($p<0.005$), and Dorfin and Dorfin-CHIP^{L} ($p<0.05$) at 3 h, as well as between Mock and Dorfin ($p<0.05$), and Mock and Dorfin-CHIP^{L} ($p<0.05$) at 6 h after labeling. Values are the means±SE, $n=4$. Statistical analysis was done by one-way ANOVA. (C) Pulse-chase analysis of SOD1^{G93A} with Dorfin-CHIP^{L}. N2a cells were coexpressed with SOD1^{G93A}-Myc and Mock, Dorfin, and Dorfin-CHIP^{L} as in panel A. (D) Serial changes in the amount of SOD1^{G93A} coexpressed with Mock, Dorfin, or Dorfin-CHIP^{L}. Four independent experiments were performed and the amounts of SOD1^{G93A} were plotted. There were significant differences between Mock and Dorfin ($p<0.05$) and Mock and Dorfin-CHIP^{L} ($p<0.01$) at 3 h, as well as between Mock and Dorfin ($p<0.05$), Mock and Dorfin-CHIP^{L} ($p<0.01$), and Dorfin and Dorfin-CHIP^{L} ($p<0.05$) at 6 h after labeling. Values are the means±SE, $n=4$. Statistics were done by one-way ANOVA. (E) The equivalent protein expression levels of Dorfin and Dorfin-CHIP^{L}. Half of the volume of samples used in the pulse-chase analysis of panel C at 0 h was used for immunoprecipitation using anti-Flag M2 antibody. The following SOD-PAGE analysis revealed the amounts of Dorfin and Dorfin-CHIP^{L} in the experiment shown in panel C.

cells, using [^{35}S] labeled Met/Cys. The protein levels of SOD1^{G85R} and SOD1^{G93A} declined more rapidly with Dorfin coexpression. Dorfin-CHIP^{L} remarkably declined in both SOD1^{G85R} and SOD1^{G93A} (Figs. 6A, C). Dorfin and Dorfin-CHIP^{L} had similar expression levels at 0 h of this experiment (Fig. 6E). As compared to Mock, Dorfin showed significant declines of both SOD1^{G85R} at 3 h ($p<0.001$) and 6 h ($p<0.05$) after labeling, as shown in a previous study (Niwa et al., 2002). Dorfin-CHIP^{L} also significantly accelerated the decline of SOD1^{G85R} at 3 h ($p<0.001$) and 6 h ($p<0.05$) after labeling again as compared to Mock. At 3 h after labeling, a significant difference between Dorfin-CHIP^{L} and Dorfin was present with respect to SOD1^{G85R} degradation ($p<0.05$). As compared to Dorfin, Dorfin-CHIP^{L} also tended toward accelerated SOD1^{G85R} degradation at 6 h after labeling (Fig. 6B). Similarly, Dorfin showed significant declines of SOD1^{G93A} at 3 h ($p<0.05$) and 6 h ($p<0.05$) after labeling, and Dorfin-CHIP^{L} significantly accelerated the declines of SOD1^{G93A} at 3 h ($p<0.01$) and 6 h ($p<0.01$) after labeling as compared to Mock. A significant difference between Dorfin-CHIP^{L} and Dorfin was present at 6 h in SOD1^{G93A} degradation ($p<0.05$) (Fig. 6D).

Attenuation of the toxicity of mutant SOD1 and decrease in the formation of visible aggregations of mutant SOD1 in cultured neuronal culture cells

The ability of Dorfin-CHIP chimeric proteins to attenuate mutant SOD1-related toxicity was analyzed by MTS assay using N2a cells. The expression of SOD1^{G85R}, as compared to that of SOD1^{WT}, decreased the viability of cells. Overexpression of Dorfin reversed the toxic effect of SOD1^{G85R}, whereas overexpression of CHIP did not. Dorfin-CHIP^{L} had a significantly greater rescue effect on SOD1^{G85R}-related cell toxicity than did Dorfin (Fig. 7A). We also measured the cell viability of N2a cells overexpressing Mock, Dorfin, and Dorfin-CHIP^{L} with various amounts of constructs, and found no difference in toxicity among them (Supplementary Fig. 2).

A structure that Johnston et al. (1998) called aggresome is formed when the capacity of a cell to degrade misfolded proteins is exceeded. The accumulation of mutant SOD1 induces visible macroaggregation, which is considered to be 'aggresome' in N2a cells. We examined the subcellular localizations of Dorfin, CHIP, and Dorfin-CHIP^{L} by immunostaining N2a cells expressing SOD1^{G85R}-GFP. Dorfin was localized in aggresomes with substrate proteins, as in our previous studies. Dorfin-CHIP^{L} was also seen in aggresomes, whereas the staining of CHIP was diffusely observed in the cytosol (Fig. 7B). We counted these visible aggregations with or without MG132 treatment. Dorfin decreased the number of aggregation-containing cells, as has been reported (Niwa et al., 2002), but Dorfin-CHIP^{L} did so more effectively. These effects were inhibited by the treatment of MG132 (Fig. 7C).

Discussion

E3 proteins can specifically recognize and degrade accumulating aberrant proteins, which are deeply involved in the pathogenesis of neurodegenerative disorders, including ALS (Alves-Rodrigues et al., 1998; Sherman and Goldberg, 2001; Ciechanover and Brundin, 2003). For this reason, E3 proteins are candidate molecules for use in developing therapeutic technology for neurodegenerative diseases. Dorfin is the first E3 molecule that has been found specifically to ubiquitylate mutant SOD1 proteins as well as to attenuate mutant SOD-associated toxicity in cultured neuronal cells (Niwa et al., 2002).

NEDL1, a HECT type E3 ligase, has also been reported to be a mutant SOD1-specific E3 ligase and to interact with TRAPδ and dvl1 (Miyazaki et al., 2004). It has also been reported that ubiquitylation of mutant SOD1-associated complex was enhanced by CHIP and Hsp70 *in vivo* (Urushitani et al., 2004). CHIP ubiquitylated Hsp70-holding SOD1 complexes and degraded mutant SOD1, but did not directly interact with mutant SOD1 (Urushitani et al., 2004). Among these E3 molecules, Dorfin seems to be the most potentially beneficial E3 protein for use in ALS therapy since it is the only one that has been demonstrated to reverse mutant SOD1-associated toxicity (Niwa et al., 2002). Furthermore, Dorfin has been localized in various ubiquitin-positive inclusions such as Lewy bodies (LB) in PD, as well as LB-like inclusions in sporadic ALS and glial cell bodies in multiple-system atrophy. These findings indicate that Dorfin may be involved in the pathogenesis of a broad spectrum of neurodegenerative disorders other than familial ALS (Hishikawa et al., 2003; Ito et al., 2003; Ishigaki et al., 2004).

The half-life of Dorfin^{WT} is, however, less than 1 h (Fig. 1, Table 1). The amount of Dorfin is increased in the presence of MG132, a proteasome inhibitor, indicating that Dorfin is immediately degraded in the UPS. Since the nonfunctional RING mutant form of Dorfin, Dorfin$^{C132S/C135S}$, degraded more slowly than did Dorfin^{WT}, Dorfin seemed to be degraded by auto-ubiquitylation. The degradation of Dorfin$^{C132S/C135S}$ is also inhibited by MG132, suggesting that it is degraded by endogenous Dorfin or other E3s. This immediate degradation of Dorfin is a serious problem for its therapeutic application against neurodegenerative diseases.

Several reports have shown that engineered chimera E3s are able to degrade certain substrates with high efficiency. Protac, a chimeric protein-targeting molecule, was designed to target methionine aminopeptidase-2 to Skp1-Cullin-F box complex (SCF) ubiquitin ligase complex for ubiquitylation and degradation (Sakamoto et al.,

Fig. 7. Dorfin-CHIP chimeric proteins can attenuate toxicity induced by mutant SOD1 and decrease the formation of visible aggregation of mutant SOD1 in N2a cells. (A) N2a cells were grown in 96 collagen-coated wells (5000 cells per well) and transfected with 0.15 μg of SOD1^{WT} and 0.05 μg of Mock or 0.15 μg of SOD1^{G85R} and 0.05 μg of Mock, Dorfin, CHIP, or Dorfin-CHIP^{L}. After the medium was changed, MTS assays were done at 48 h of incubation. Viability was measured as the level of absorbance (490 nm). Values are the means±SE, $n=6$. Statistics were carried out by one-way ANOVA. There were significant differences between SOD1^{G85R}-expressing cells coexpressed with Mock and SOD1^{G85R}-expressing cells coexpressed with Dorfin ($p<0.001$), as well as between SOD1^{G85R}-expressing cells coexpressed with Dorfin and SOD1^{G85R}-expressing cells coexpressed with Dorfin-CHIP^{L} ($p<0.001$). (B) N2a cells were transiently expressed with SOD1^{G85R}-GFP and Mock, Dorfin, CHIP, or Dorfin-CHIP^{L}. Immunostaining with anti-FLAG antibody revealed that Dorfin, CHIP, and Dorfin-CHIP^{L} were localized with SOD1^{G85R}-GFP in macroaggresomes (arrows). Scale bar=20 μm (C) The visible macroaggregations in N2a cells expressing both SOD1^{G85R}-GFP and Mock, Dorfin, CHIP, or Dorfin-CHIP^{L} with or without MG132 treatment were counted and the ratio of cells with aggregations to those with GFP signals was calculated. Values are the means±SE, $n=4$. Statistics were done by one-way ANOVA. *$p<0.01$ denotes a significant difference between cells with Mock and Dorfin or Dorfin-CHIP^{L}. **$p<0.05$ denotes a significant difference between cells with Dorfin and Dorfin-CHIP^{L}.

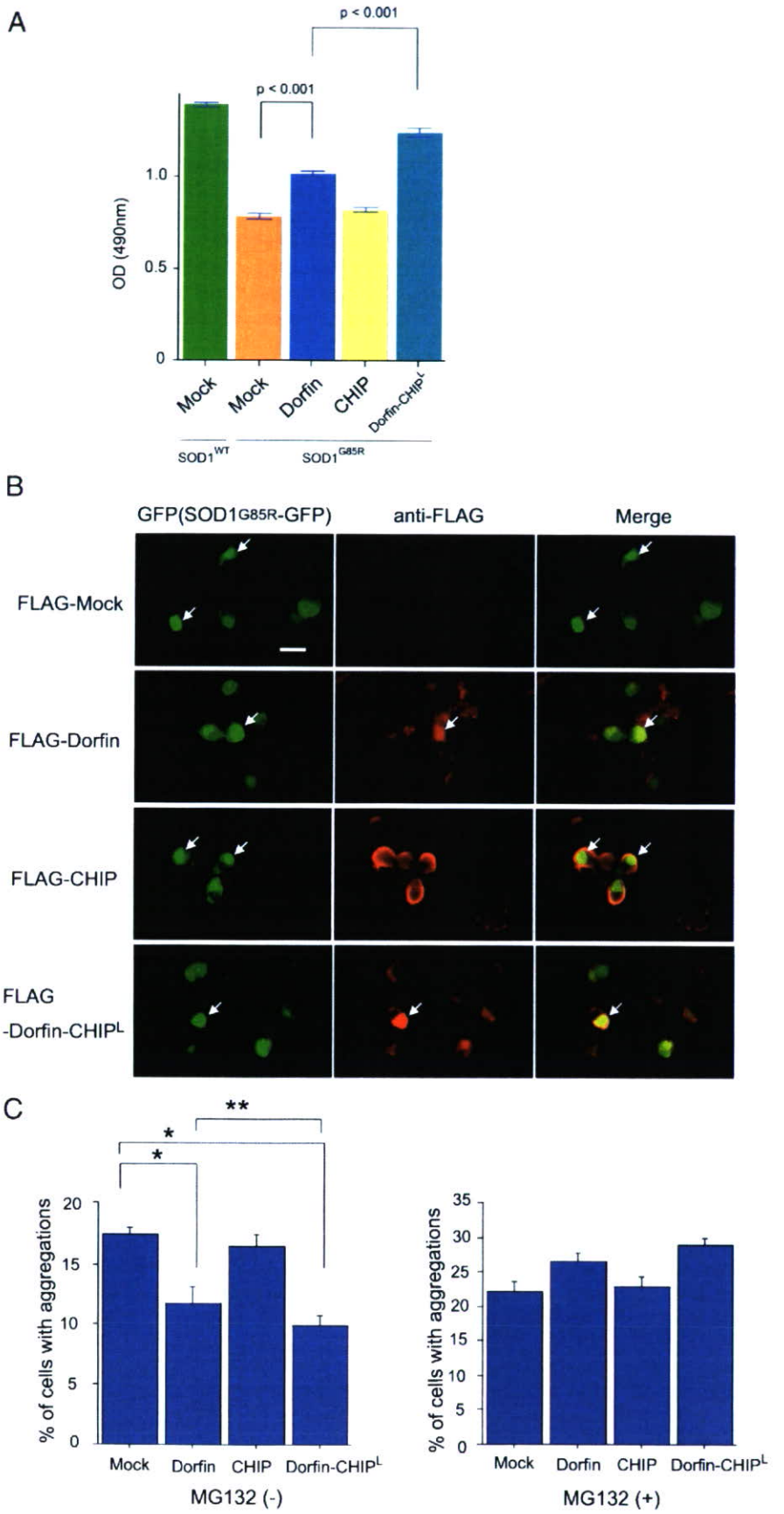
A
p < 0.001
p < 0.001
OD (490nm)
1.0
0.5
0
Mock
Mock
Dorfin
CHIP
Dorfin-CHIP^L
SOD1^WT
SOD1^G85R
B
GFP(SOD1G85R-GFP)
anti-FLAG
Merge
FLAG-Mock
FLAG-Dorfin
FLAG-CHIP
FLAG
-Dorfin-CHIP^L
C
**
*
*
% of cells with aggregations
20
15
10
5
0
Mock
Dorfin
CHIP
Dorfin-CHIP^L
MG132 (-)
35
30
25
20
15
10
5
0
Mock
Dorfin
CHIP
Dorfin-CHIP^L
MG132 (+)

2001, 2003). Oyake et al. (2002) developed double RING ubiquitin ligases containing the RING finger domains of both BRCA and BARD1 linked to a substrate recognition site PCNA. Recently, Hatakeyama et al. developed a fusion protein composed of Max, which forms a heterodimer with c-Myc, and the U-box of CHIP. This fusion protein physically interacted with c-Myc and promoted the ubiquitylation of c-Myc. It also reduced the stability of c-Myc, resulting in the suppression of transcriptional activity dependent on c-Myc and the inhibition of tumorogenesis (Hatakeyama et al., 2005). This indicated that the U-box portion of CHIP is able to add an effective E3 function to a U-box-containing client protein.

We postulated that engineered forms of Dorfin could be stable and still function as specific E3s for mutant SOD1s. Dorfin has a RING/IBR domain in the N-terminal portion (amino acids 1-332), but has no obvious motif in the rest of the C-terminus (amino acids 333–838). In this study, we have demonstrated that the hydrophobic domain of Dorfin (amino acids 333–454) is both necessary and sufficient for substrate recruiting (Fig. 2B). In our engineered proteins, the RING/IBR motif of N-terminal Dorfin was replaced by the UPR domain of CHIP, which had strong E3 activity (Murata et al., 2001). Some of the engineered Dorfin-chimeric proteins, such as Dorfin-CHIP$^{D, G, J}$, and ^{L}, were degraded *in vivo* far more slowly than was wild-type Dorfin, indicating that they were capable of being stably presented *in vivo* (Fig. 3). However, Dorfin-CHIP^{G} failed to show strong ubiquitylation activity against SOD1^{G85R} in HEK293 cells. Since Dorfin-CHIP$^{D, J}$, and ^{L} were able to bind to SOD1^{G85R} more strongly than did Dorfin-CHIP^{G}, the binding activity was more important for the E3 activity than for the protein stability.

We next showed that although all of the Dorfin-CHIP chimeric proteins bound to mutant SOD1 *in vivo*, some of them, such as Dorfin-CHIP$^{B, C}$, and ^{I}, bound less than others (Fig. 4A). In HEK293 cells, Dorfin-CHIP$^{D, E, F, J, K}$, and ^{L} ubiquitylated SOD1^{G85R} more effectively than did Dorfin or CHIP; however, in N2a cells only Dorfin-CHIP^{L} had more effective E3 activity than did Dorfin or CHIP. This discrepancy may be due to differences between HEK 293 and N2a cells which could provide slight different environment for the E3 machinery. Therefore, Dorfin-CHIP^{L} was the most potent of the candidate chimeric proteins in degrading mutant SOD1 in the UPS in neuronal cells. We also showed that Dorfin-CHIP^{L} could specifically bind to and ubiquitylate mutant SOD1s but not SOD1^{WT} *in vivo*, as Dorfin had done (Niwa et al., 2002; Ishigaki et al., 2004) (Fig. 5). This observation confirmed that the hydrophobic domain of Dorfin (amino acids 333–454) is responsible for mutant SOD1 recruiting.

Pulse-chase analysis using N2a cells showed that Dorfin-CHIP^{L} degraded SOD1^{G85R} and SOD1^{G93A} more effectively than did Dorfin (Fig. 6). This is compatible with the finding that Dorfin-CHIP^{L} had a greater effect than Dorfin did on the ubiquitylation against mutant SOD1. The cycloheximide assay verified that the degradation ability of Dorfin-CHIP^{L} against SOD1^{G85R} was stronger than that of Dorfin or CHIP in HEK293 cells (data not shown).

Dorfin-CHIP^{L} also reversed SOD1^{G85R}-associated toxicity in N2a cells more effectively than did Dorfin (Fig. 7). This therapeutic effect of Dorfin-CHIP^{L} was expected from its strong E3 activity and degradation ability against SOD1^{G85R}. Visible protein aggregations have been considered to be hallmarks of neurodegeneration. Increased understanding of the pathway involved in protein aggregation may demonstrate that visible macroaggregates represent the end-stage of a molecular cascade of steps rather than a direct toxic insult (Ross and Poirier, 2004). Two facts that Dorfin-CHIP^{L} decreased aggregation formation of SOD1^{G85R} and that this effect was inhibited by a proteasome inhibitor should reflect the ability of Dorfin-CHIP^{L} to degrade mutant SOD1 in the UPS of cells.

Based on our present observations, Dorfin-CHIP^{L}, an engineered chimeric molecule with the hydrophobic substrate-binding domain of Dorfin and the U-box domain of CHIP, had stronger E3 activity against mutant SOD1 than did Dorfin or CHIP. Indeed, it not only degraded mutant SOD1 more effectively than did Dorfin or CHIP but, as compared to Dorfin, produced marked attenuation of mutant SOD1-associated toxicity in N2a cells. This protective effect of Dorfin-CHIP^{L} against mutant SOD1 has potential applications to gene therapy for mutant SOD1 transgenic mice because this protein has a long enough life to allow the constant removal of mutant SOD1 from neurons. Since Dorfin was originally identified as a sporadic ALS-associated molecule (Ishigaki et al., 2002b) and is located in the ubiquitin-positive inclusions of various neurodegenerative diseases (Hishikawa et al., 2003), this molecule is an appropriate candidate for future use in gene therapy not only for familial ALS, but also for sporadic ALS and other neurodegenerative disorders.

So far, most reports on engineered chimera E3s have targeted cancer-promoting proteins. Dorfin-CHIP chimeric proteins are the first chimera E3s to be intended for the treatment of neurodegenerative diseases. Since the accumulation of ubiquitylated proteins in neurons is a pathological hallmark of various neurodegenerative diseases, development of chimera E3s like Dorfin-CHIP^{L}, which can remove unnecessary proteins, is a new therapeutic concept. Further analysis, including transgenic overexpression and vector delivery of Dorfin-CHIP chimeric proteins using ALS animal models will increase our understanding of the potential utility of Dorfin-CHIP chimeric proteins as therapeutic tools.

Acknowledgments

We gratefully thank Dr. Shigetsugu Hatakeyama at Hokkaido University for his advice about the construction of Dorfin-CHIP chimeric proteins. This work was supported by the Nakabayashi Trust for ALS Research; a grant for Center of Excellence (COE) from the Ministry of Education, Culture, Sports, Science and Technology of Japan; and grants from the Ministry of Health, Welfare and Labor of Japan.

Appendix A. Supplementary data

Supplementary data associated with this article can be found, in the online version, at doi:10.1016/j.nbd.2006.09.017.

References

Alves-Rodrigues, A., Gregori, L., Figueiredo-Pereira, M.E., 1998. Ubiquitin, cellular inclusions and their role in neurodegeneration. Trends Neurosci. 21, 516–520.

Bercovich, B., Stancovski, I., Mayer, A., Blumenfeld, N., Laszlo, A., Schwartz, A.L., Ciechanover, A., 1997. Ubiquitin-dependent degradation of certain protein substrates in vitro requires the molecular chaperone Hsc70. J. Biol. Chem. 272, 9002–9010.

Ciechanover, A., Brundin, P., 2003. The ubiquitin proteasome system in

neurodegenerative diseases: sometimes the chicken, sometimes the egg. Neuron 40, 427–446.

Cudkowicz, M.E., McKenna-Yasek, D., Sapp, P.E., Chin, W., Geller, B., Hayden, D.L., Schoenfeld, D.A., Hosler, B.A., Horvitz, H.R., Brown, R.H., 1997. Epidemiology of mutations in superoxide dismutase in amyotrophic lateral sclerosis. Ann. Neurol. 41, 210–221.

Glickman, M.H., Ciechanover, A., 2002. The ubiquitin–proteasome proteolytic pathway: destruction for the sake of construction. Physiol. Rev. 82, 373–428.

Hatakeyama, S., Matsumoto, M., Kamura, T., Murayama, M., Chui, D.H., Planel, E., Takahashi, R., Nakayama, K.I., Takashima, A., 2004. U-box protein carboxyl terminus of Hsc70-interacting protein (CHIP) mediates poly-ubiquitylation preferentially on four-repeat Tau and is involved in neurodegeneration of tauopathy. J. Neurochem. 91, 299–307.

Hatakeyama, S., Watanabe, M., Fujii, Y., Nakayama, K.I., 2005. Targeted destruction of c-Myc by an engineered ubiquitin ligase suppresses cell transformation and tumor formation. Cancer Res. 65, 7874–7879.

Hishikawa, N., Niwa, J., Doyu, M., Ito, T., Ishigaki, S., Hashizume, Y., Sobue, G., 2003. Dorfin localizes to the ubiquitylated inclusions in Parkinson's disease, dementia with Lewy bodies, multiple system atrophy, and amyotrophic lateral sclerosis. Am. J. Pathol. 163, 609–619.

Ishigaki, S., Liang, Y., Yamamoto, M., Niwa, J., Ando, Y., Yoshihara, T., Takeuchi, H., Doyu, M., Sobue, G., 2002a. X-Linked inhibitor of apoptosis protein is involved in mutant SOD1-mediated neuronal degeneration. J. Neurochem. 82, 576–584.

Ishigaki, S., Niwa, J., Ando, Y., Yoshihara, T., Sawada, K., Doyu, M., Yamamoto, M., Kato, K., Yotsumoto, Y., Sobue, G., 2002b. Differentially expressed genes in sporadic amyotrophic lateral sclerosis spinal cords—Screening by molecular indexing and subsequent cDNA microarray analysis. FEBS Lett. 531, 354–358.

Ishigaki, S., Hishikawa, N., Niwa, J., Iemura, S., Natsume, T., Hori, S., Kakizuka, A., Tanaka, K., Sobue, G., 2004. Physical and functional interaction between Dorfin and Valosin-containing protein that are colocalized in ubiquitylated inclusions in neurodegenerative disorders. J. Biol. Chem. 279, 51376–51385.

Ito, T., Niwa, J., Hishikawa, N., Ishigaki, S., Doyu, M., Sobue, G., 2003. Dorfin localizes to Lewy bodies and ubiquitylates synphilin-1. J. Biol. Chem. 278, 29106–29114.

Johnston, J.A., Ward, C.L., Kopito, R.R., 1998. Aggresomes: a cellular response to misfolded proteins. J. Cell Biol. 143, 1883–1898.

Julien, J.P., 2001. Amyotrophic lateral sclerosis. unfolding the toxicity of the misfolded. Cell 104, 581–591.

Jungmann, J., Reins, H.A., Schobert, C., Jentsch, S., 1993. Resistance to cadmium mediated by ubiquitin-dependent proteolysis. Nature 361, 369–371.

Lee, D.H., Sherman, M.Y., Goldberg, A.L., 1996. Involvement of the molecular chaperone Ydj1 in the ubiquitin-dependent degradation of short-lived and abnormal proteins in *Saccharomyces cerevisiae*. Mol. Cell. Biol. 16, 4773–4781.

Meacham, G.C., Patterson, C., Zhang, W., Younger, J.M., Cyr, D.M., 2001. The Hsc70 co-chaperone CHIP targets immature CFTR for proteasomal degradation. Nat. Cell Biol. 3, 100–105.

Miyazaki, K., Fujita, T., Ozaki, T., Kato, C., Kurose, Y., Sakamoto, M., Kato, S., Goto, T., Itoyama, Y., Aoki, M., Nakagawara, A., 2004. NEDL1, a novel ubiquitin–protein isopeptide ligase for dishevelled-1, targets mutant superoxide dismutase-1. J. Biol. Chem. 279, 11327–11335.

Murata, S., Minami, Y., Minami, M., Chiba, T., Tanaka, K., 2001. CHIP is a chaperone-dependent E3 ligase that ubiquitylates unfolded protein. EMBO Rep. 2, 1133–1138.

Murata, S., Chiba, T., Tanaka, K., 2003. CHIP: a quality-control E3 ligase collaborating with molecular chaperones. Int. J. Biochem. Cell Biol. 35, 572–578.

Niwa, J., Ishigaki, S., Doyu, M., Suzuki, T., Tanaka, K., Sobue, G., 2001. A novel centrosomal ring-finger protein, dorfin, mediates ubiquitin ligase activity. Biochem. Biophys. Res. Commun. 281, 706–713.

Niwa, J., Ishigaki, S., Hishikawa, N., Yamamoto, M., Doyu, M., Murata, S., Tanaka, K., Taniguchi, N., Sobue, G., 2002. Dorfin ubiquitylates mutant SOD1 and prevents mutant SOD1-mediated neurotoxicity. J. Biol. Chem. 277, 36793–36798.

Oyake, D., Nishikawa, H., Koizuka, I., Fukuda, M., Ohta, T., 2002. Targeted substrate degradation by an engineered double RING ubiquitin ligase. Biochem. Biophys. Res. Commun. 295, 370–375.

Rosen, D.R., Siddique, T., Patterson, D., Figlewicz, D.A., Sapp, P., Hentati, A., Donaldson, D., Goto, J., O'Regan, J.P., Deng, H.X., et al., 1993. Mutations in Cu/Zn superoxide dismutase gene are associated with familial amyotrophic lateral sclerosis. Nature 362, 59–62.

Ross, C.A., Poirier, M.A., 2004. Protein aggregation and neurodegenerative disease. Nat. Med. 10, S10–S17 (Suppl.).

Rowland, L.P., Shneider, N.A., 2001. Amyotrophic lateral sclerosis. N. Engl. J. Med. 344, 1688–1700.

Sakamoto, K.M., Kim, K.B., Kumagai, A., Mercurio, F., Crews, C.M., Deshaies, R.J., 2001. Protacs: chimeric molecules that target proteins to the Skp1-Cullin-F box complex for ubiquitination and degradation. Proc. Natl. Acad. Sci. U. S. A. 98, 8554–8559.

Sakamoto, K.M., Kim, K.B., Verma, R., Ransick, A., Stein, B., Crews, C.M., Deshaies, R.J., 2003. Development of Protacs to target cancer-promoting proteins for ubiquitination and degradation. Mol. Cell Proteomics 2, 1350–1358.

Scheffner, M., Nuber, U., Huibregtse, J.M., 1995. Protein ubiquitination involving an E1–E2–E3 enzyme ubiquitin thioester cascade. Nature 373, 81–83.

Sherman, M.Y., Goldberg, A.L., 2001. Cellular defenses against unfolded proteins: a cell biologist thinks about neurodegenerative diseases. Neuron 29, 15–32.

Shimura, H., Schwartz, D., Gygi, S.P., Kosik, K.S., 2004. CHIP–Hsc70 complex ubiquitinates phosphorylated tau and enhances cell survival. J. Biol. Chem. 279, 4869–4876.

Tanaka, K., Suzuki, T., Hattori, N., Mizuno, Y., 2004. Ubiquitin, proteasome and parkin. Biochim. Biophys. Acta 1695, 235–247.

Urushitani, M., Kurisu, J., Tateno, M., Hatakeyama, S., Nakayama, K., Kato, S., Takahashi, R., 2004. CHIP promotes proteasomal degradation of familial ALS-linked mutant SOD1 by ubiquitinating Hsp/Hsc70. J. Neurochem. 90, 231–244.

Yoshida, Y., Tokunaga, F., Chiba, T., Iwai, K., Tanaka, K., Tai, T., 2003. Fbs2 is a new member of the E3 ubiquitin ligase family that recognizes sugar chains. J. Biol. Chem. 278, 43877–43884.

Available online at www.sciencedirect.com
ScienceDirect
Behavioural Brain Research 185 (2007) 110–118
BEHAVIOURAL BRAIN RESEARCH
www.elsevier.com/locate/bbr

Research report

Alteration of behavioural phenotype in mice by targeted disruption of the progranulin gene

Yuko Kayasuga [a], Shuichi Chiba [a], Masatoshi Suzuki [a], Takefumi Kikusui [b], Takashi Matsuwaki [a], Keitaro Yamanouchi [a], Hayato Kotaki [c], Reiko Horai [c], Yoichiro Iwakura [c], Masugi Nishihara [a,*]

[a] *Department of Veterinary Physiology, Veterinary Medical Science, The University of Tokyo, 1-1-1 Yayoi, Bunkyo-ku, Tokyo 113-8657, Japan*
[b] *Department of Veterinary Ethology, Animal Resource Science, The University of Tokyo, Tokyo 113-8657, Japan*
[c] *Division of Cell Biology, Center for Experimental Medicine, Institute of Medical Science, The University of Tokyo, Tokyo 108-8639, Japan*

Received 30 March 2007; received in revised form 12 July 2007; accepted 15 July 2007
Available online 20 July 2007

Abstract

Sexual differentiation of the brain in rodents is achieved by estrogens, which are converted from androgens in the brain, during the perinatal period. We have identified the progranulin (PGRN) gene as one of the sex steroid-inducible genes that may be involved in masculinization of the rat brain. In the present study, we generated a line of mice with targeted disruption of the PGRN gene, and investigated male sexual behaviour, aggression and anxiety. PGRN-deficient mice exhibited a decrease in ejaculation incidence, while the latency and frequency of both mount and intromission were unchanged. For the aggressive behaviour test, the resident–intruder paradigm was used, and PGRN-deficient mice exhibited enhanced aggressiveness. In wild-type mice, males exhibited lower levels of anxiety than females by the open field test, while male PGRN-deficient mice exhibited an elevated level of anxiety and sex difference in anxiety was not observed. In addition, mRNA expression of the serotonergic receptor 5-HT1A, which could be related to the inhibition of aggression and anxiety, was significantly reduced in the hippocampus of PGRN-deficient mice after aggressive encounters. On the other hand, deficiency of the PGRN gene did not affect serum testosterone concentrations. These results suggest that PGRN gene plays a role in establishing sexual dimorphic behaviours at least partially by modulating the brain serotonergic system.
© 2007 Elsevier B.V. All rights reserved.

Keywords: Aggression; Anxiety; Frontotemporal dementia; Gene targeting; Progranulin; Sexual behaviour; Sexual differentiation

1. Introduction

It is well established that the mammalian brain possesses sexually dimorphic structure, which is reflected by functional sexual differences in the control of specific types of behaviour and endocrine patterns [1]. In rodent species, such as rats and mice, sexual dimorphism of the brain is established during the perinatal period, which is known as the critical period for brain sexual differentiation. During this period, androgens secreted from the testis masculinize the brain in males, while the female brain is not exposed to androgens and thereby develops into the "default" female type. In the brain, androgens are converted to estrogens by aromatase and are then involved in the masculinization of the brain through the facilitation of transcription of various factors [32].

In an attempt to identify genes that are involved in sexual differentiation of the brain, we have isolated the progranulin (PGRN) gene as an androgen-inducible gene in neonatal rat hypothalamus [45]. The expression of PGRN mRNA in the hypothalamus of males is maintained at high levels throughout the critical period, yet abruptly declines in females after birth. As estrogens can induce PGRN gene expression in the hypothalamus [48], androgens probably induce PGRN gene expression after being converted to estrogens. We further observed that infusion of an antisense oligodeoxynucleotide for the PGRN gene into the neonatal male rat brain significantly suppressed male sexual behaviours after maturation [46], suggesting that the PGRN gene is indeed involved in the process of masculin-

* Corresponding author. Tel.: +81 3 5841 5386; fax: +81 3 5841 8017.
E-mail address: amnishi@mail.ecc.u-tokyo.ac.jp (M. Nishihara).

0166-4328/$ – see front matter © 2007 Elsevier B.V. All rights reserved.
doi:10.1016/j.bbr.2007.07.020

ization of the rat brain. Recently, we have also found that PGRN is involved in estrogen-induced neurogenesis in the adult rat hippocampus [11].

In the mouse, the PGRN gene spans approximately 6.3 kbp and contains 13 exons [3]. PGRN mRNA has been demonstrated in various tissues and organs including the reproductive organs, gastrointestinal tract, endocrinal organs and neural tissues [9,17]. Peptides of approximately 6 kDa called granulins [6,8] also known as epithelins [42] are derived from PGRN. Both PGRN and granulins have growth-modulating effects on many cell types in culture [7,42]. For example, PGRN mediates the mitogenic effect of estrogens on MCF-7 cells, a human breast cancer cell line [30], which supports the above-mentioned notion that transcription of the PGRN gene is induced by estrogens. In addition, it has been recently reported that mutations in PGRN cause tau-negative, ubiquitin-positive frontotemporal dementia (FTD) in humans [4,16], suggesting that PGRN is involved in neuronal survival.

To elucidate the physiological roles of PGRN/granulins *in vivo*, especially their roles in the brain, we generated mice lacking the PGRN gene in the present study. Here, we describe their phenotypes regarding sexually dimorphic behaviours, such as sexual behaviour, aggression and anxiety.

2. Materials and methods

2.1. Generation of mice lacking the PGRN gene

A PGRN genomic clone was isolated from the 129 SvJ mouse genomic library (Stratagene, La Jolla, CA). The targeting vector was constructed by replacing an internal 4.7 kb EcoRV–EcoRI fragment, encoding exons 2–13 of the PGRN gene, with a PGK-Neo-bpA cassette [43] and by ligating the diphtheria toxin A (DT-A) fragment [54] to the 5′ end of the vector (Fig. 1A). The neomycin resistance gene, under the control of the phosphoglycerate kinase (PGK) 1 promoter, was inserted as a positive selection marker and DT-A fragment DNA, under the polyoma enhancer/herpes simplex virus thymidine promoter (MC-1), was used as a negative selection mechanism for the screening of recombinant embryonic stem (ES) cells. The targeting vector, linearized by ApaI, was electroporated (250 V, 5 μF) into 10^7 E14.1 ES cells [22], which were then selected with 250 μg/ml G418 (Gibco BRL, Grand Island, NY) for 7 days, as previously described [2]. Homologous recombination was confirmed by Southern blot analysis, as described below. For the generation of chimeric mice, ES cells were aggregated with two (C57BL/6 × DBF_1)

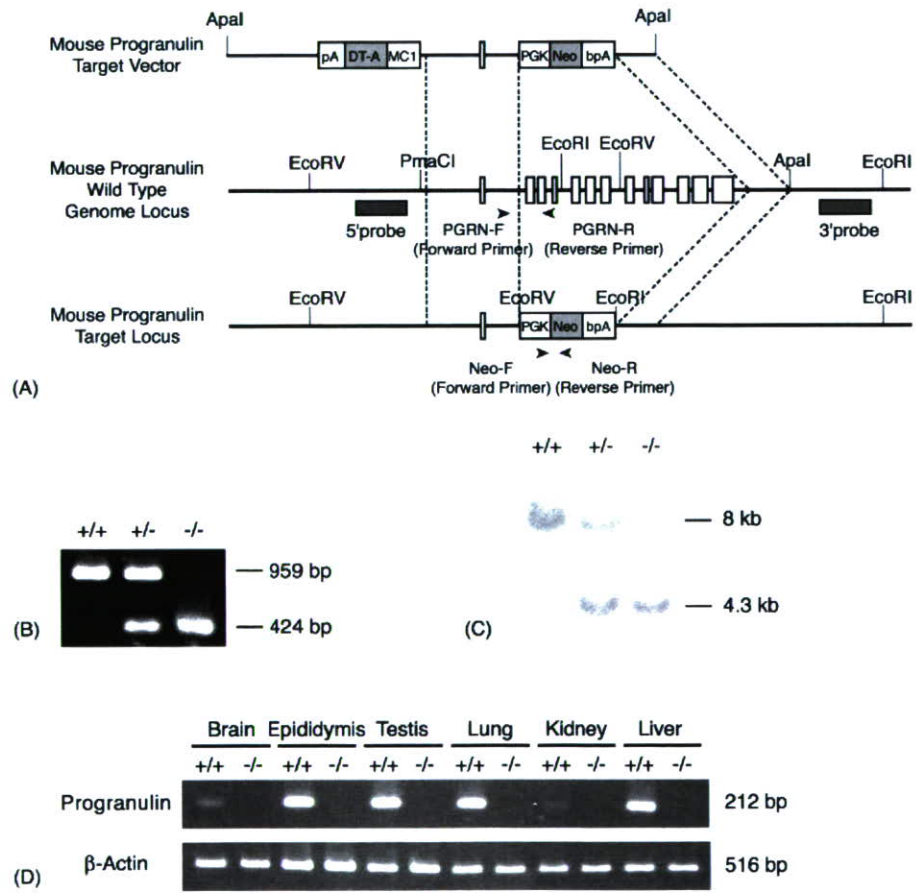

Fig. 1. Generation of mice with targeted disruption of the PGRN gene. (A) The targeting strategy for the mouse genomic PGRN locus. Construct of the targeting vector used to knockout the PGRN gene (top), the wild-type genome locus of mouse PGRN (middle) and the recombinated gene locus (bottom). In the mutant locus, the genomic region from exon 2 to exon 13 was replaced by the PGK-Neo-bpA cassette. The arrowheads indicate the location of the primers for PCR analysis and the grey boxes indicate the 5′ and 3′ probes for Southern blot analyses. Restriction enzyme sites used for linearization of the vector and Southern blot analyses are also indicated. (B) Bands detected in the PCR analysis of DNA from the tail of mice bred by $Grn^{+/-}$ intercrossing. The PCR products sized 959 bp correspond to the wild-type gene and the 424 bp bands correspond to the mutant gene. (C) Bands detected by Southern blot analysis using the 3′ probe following EcoRI digestion of genomic DNA from the tail of mice bred by $Grn^{+/-}$ intercrossing. The 8 kb fragment corresponds to the wild-type genome locus and the 4.3 kb bands correspond to the mutant genome locus. (D) PGRN gene expression in $Grn^{+/+}$ and $Grn^{-/-}$ mice. Total RNA was isolated from the brain, testis, epididymis, kidney, lung and liver of adult male $Grn^{+/+}$ and $Grn^{-/-}$ mice. The 212 bp bands correspond to PGRN and the 516 bp bands correspond to β-actin.

F_1 eight cell stage embryos, according to the method described previously [23].

Genotyping of offspring was carried out by PCR and Southern blot analysis with genomic DNA extracted from the tail of mice. The locus of PCR primers and probes, as well as the pattern diagrams of the targeting vector, are shown in Fig. 1A. The extraction of DNA for PCR and the PCR reactions were performed with a REDExtract-N-Amp Tissue PCR Kit (Sigma, Saint Louis, MO). The mutant gene was detected with the primers Neo-F (CCA ATA TGG GAT CGG CCA TTG AAC) and Neo-R (CGC TCG ATG CGA TGT TTC GCT TGG) and the wild-type (WT) gene with the primers PGRN-F (CAT GTG ACT GAT GAC TGT CC) and PGRN-R (GAG CAA GAC GCT TTT GCT TG). PCR reactions were carried out as follows: at 94 °C for 3 min for the initial denaturation, then 35 cycles at 94 °C for 30 s, 58 °C for 30 s and 72 °C for 30 s for amplification and 72 °C for 10 min for the final extension. Southern blot analysis was performed as previously reported [54]. Genomic DNA extracted from ES cell clones or mouse-tails were digested by EcoRV and EcoRI for the 5′ and 3′ probes flanking the targeting vector, respectively.

For RT-PCR, total RNA was isolated from the brain, testis, epididymis, kidney, lung and liver of adult wild-type ($Grn^{+/+}$) and PGRN-deficient ($Grn^{-/-}$) mice using TRIzol reagent (Gibco BRL, Grand Island, NY). First-strand cDNA was synthesized using Superscript II (Invitrogen, Carlsbad, CA) with oligo $d(T)_{16}$ primers (Roche, Mannheim, Germany). The forward and reverse primers used for PGRN were AGT TCG AAT GTC CTG ACT CCG CCA and AAG CCA CTG CCC TGT TGG TCC TTT, respectively, and those for β-actin (as positive control) were TCA GAA GGA CTC CTA TGT GG and GCA ACA TAG CAC AGC TTC TC, respectively. The PCR reactions were carried out in the following way: 10 min at 95 °C for initial denaturation, then 30 cycles at 94 °C for 45 s, 60 °C for 30 s and 72 °C for 1 min 45 s for amplification.

2.2. Animal care

All animal care and experiments were performed according to the guidelines for the Care and Use of Laboratory Animals, Graduate School of Agricultural and Life Sciences, the University of Tokyo. C57BL/6J and A/J mice were purchased from Sankyo Laboratory (Tokyo, Japan). Mice were group-housed in plastic cages and maintained on a 12 h light:12 h dark cycle (lights on at 07:00 h) at constant temperature (22–24 °C). Food (Lab MR Stock, Nihon Nousan Kougyou, Kanagawa, Japan) and water were available *ad libitum*. The line of the PGRN KO mouse was maintained by backcrossing $Grn^{+/-}$ males to C57BL/6J females. To breed the animals for the experiments, $Grn^{+/-}$ males were mated with $Grn^{+/-}$ females so that offspring with all genotypes were obtained in the same litter. In the experiment to compare litter size, $Grn^{+/+}$ and $Grn^{-/-}$ males were mated with $Grn^{+/+}$ and $Grn^{-/-}$ females, respectively. Pups were weaned at 30 days of age and tail tissue sampled for genotyping. Some of the adult males (11 weeks old), which had not been used for any other experiments, were sacrificed by decapitation under ether anesthesia and blood samples collected. Serum was separated and stored at −80 °C until assayed for testosterone. Serum concentrations of testosterone were determined with a testosterone EIA kit (Cayman Chemical, Ann Arbor, MI).

2.3. Behavioural analyses

Male sexual behaviour, aggression and anxiety were investigated using the mice at the age of 7–11 weeks. For each behavioural experiment, separate groups of mice were used. In the male sexual behaviour test, each male was isolated 1 h before the test, and tested for 1 h with a sexually naive C57BL/6J female mouse. All the stimulus females were ovariectomized and subcutaneously injected with 20 μg 17β-estradiol (48 and 24 h before the test) and 500 μg progesterone (4 h before the test) to ensure high sexual receptivity. The behaviour was videotaped and the numbers and latencies of mount and intromission were recorded. The incidence of ejaculation (percentage of animals that ejaculated) was determined by the existence of vaginal plugs in the females after each test. Aggressive behaviours toward females were also recorded. An aggressive bout was defined as a continuous series of behavioural interactions including at least one aggressive behavioural act, i.e., biting, aggressive grooming and tail rattling. If the interval between the occurrences of two aggressive behavioural acts exceeded 3 s, the behavioural act was scored as two separate aggressive bouts. The tests were performed between 20:00 and 21:00 h, and repeated three times for each male at 4-day intervals.

For the aggressive behaviour test, the resident–intruder paradigm [35] was used. Each male was isolated 1 h before the test and tested in his home cage (as a resident) against a group-housed (6–8 mice per cage) male A/J intruder mouse, and the behaviour videotaped for up to 15 min. Latency to the first biting attack and the number of biting attacks during a 5 min period after the first attack were recorded. When mice did not show any biting behaviour for 10 min, the test was stopped and the latency regarded as 10 min. The tests were performed between 12:00 and 16:00 h, and repeated three times for each male at 3-day intervals. Each male encountered a novel intruder at every trial. To evaluate locomotor activity during the test, the duration of walking and the number of rearings was recorded for 5 min after the first attack in the first trial. When there was no biting, the latter 5 min of the 10-min period videotaped was used to evaluate locomotor activity.

To evaluate anxiety, the open field test was performed. The mice were moved to the experimental room more than 1 h before the start of the test. The open field was composed of 50 cm × 50 cm surrounded by 40-cm-high wooden walls painted white. The tests were performed between 13:00 and 17:00 h, and the area was cleaned between mice. Each mouse was introduced in the center of the square and its behaviour was recorded on videotape for 10 min. The duration when the mouse stayed in the peripheral zone (7.5 cm from the wall) or the center, and the distance traveled and incidence of rearings in either area, were analyzed using a computerized technique with ethovision 3.0 (Noldus, Wageningen, Netherlands).

2.4. Quantitative real-time PCR

Using different groups of mice from those used for behavioural tests mentioned above, 5-hydoroxytriptamine receptor 1A (5-HT1A) and 5-HT1B mRNA levels in the hippocampus were determined after aggressive encounters. Male mice of each genotype were isolated from their home cages 1 h before the encounter with male A/J intruder mice. The behaviour was observed for 15 min and whether the intruder was attacked or not was checked. The encounters were repeated three times for each male at 2- or 3-day intervals. Control mice were similarly isolated three times but did not encounter any intruders. Right after the third test, mice were sacrificed and total RNA was isolated from the hippocampus. RNA isolation and first-strand cDNA synthesis were done as described above. Then real-time PCR was performed using the cDNA as a template. PCR reactions were performed with QuantiTect SYBR Green PCR (Qiagen, Hilden, Germany) and a Light Cycler (Roche, Mannheim, Germany). The forward and reverse primers used for 5-HT1A were TCG CTC ACT TGG CTC ATT GGC TTT and TTC CAA CTT CTT GAC CGT CTT GCG, respectively, and those for 5-HT1B were GCT GGA CTG CTT TGT GAA CAC CGA and AAT GGA GGT GAC CGA GGA TGT GGA, respectively. The forward and reverse primers used for hypoxanthine phosphoribosyltransferase (HPRT; as an internal standard) were CTT GAG CAC ACA GAG GGC CAC AAT and AGT CCC AGC GTC GTG ATT AGC GAT, respectively. The PCR reactions were carried out in the following way for 5-HT1A and HPRT: 15 min at 95 °C for the initial denaturation, then 35 cycles at 95 °C for 30 s, 60 °C for 20 s and 72 °C for 20 s for amplification, and for 5-HT1B: 15 min at 95 °C for the initial denaturation, then 35 cycles at 95 °C for 15 s, 60 °C for 30 s and 72 °C for 20 s for amplification.

2.5. Statistical analyses

Except for the incidence of ejaculation, the data from the behavioural analyses, and 5-HT mRNA expression analyses were analyzed by repeated or non-repeated two-way analysis of variance (ANOVA) followed by post hoc comparison with Fisher's PLSD or Holm's test. The incidence of ejaculation data was analyzed by Fisher's exact probability test. The data from other experiments were analyzed by ANOVA followed by post hoc comparison with Fisher's PLSD test. The differences were considered statistically significant at $p < 0.05$.

3. Results

3.1. Generation of mice lacking the PGRN gene

We cloned the mouse PGRN gene and disrupted it in an ES cell line derived from the 129 SvJ mouse strain (Fig. 1A). Six targeted clones out of 547 were identified by Southern blot analysis and 3 of these (6D5, 18C4 and 19B2) had normal karyotypes and were used for the production of chimeric mice. The chimeric mice were mated with C57BL/6 females. One of the chimeras, 6D5-#6 was shown to be a germ line chimera and heterozygous offspring obtained from him were backcrossed to C57BL/6 females. Genotyping was carried out by PCR analysis with genomic DNA extracted from the tail. We detected bands of 959 bp using genomic DNA obtained from wild-type ($Grn^{+/+}$) mice as a template, a band of 424 bp from homozygous ($Grn^{-/-}$) mice and two bands of 959 and 424 bp from heterozygous ($Grn^{+/-}$) mice (Fig. 1B). To confirm the results of the PCR analysis, Southern blot analysis was also performed. Fig. 1C shows the result of Southern blot analysis using the 3′ probe

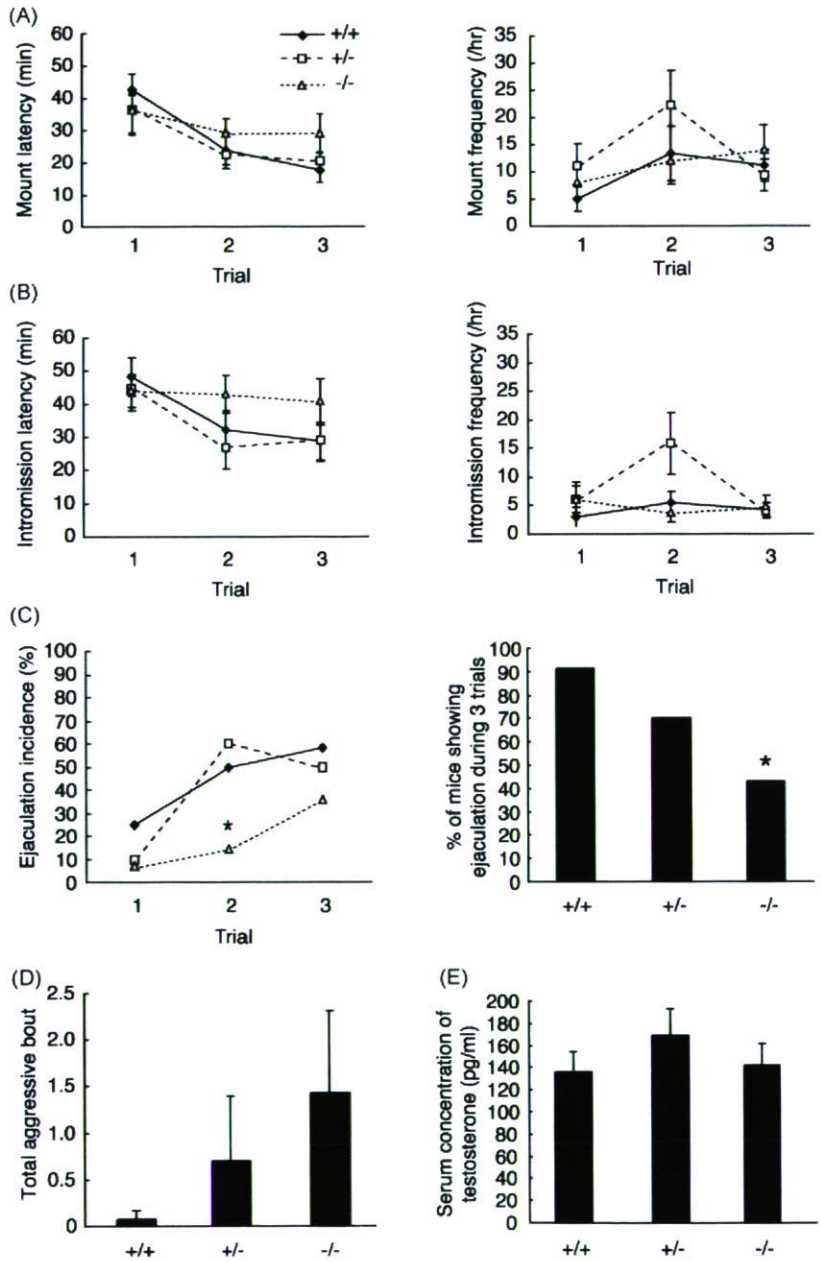

Fig. 2. Analysis of male sexual behaviour. Each male was tested for 1 h with a stimulus female and behaviour recorded. Tests were repeated three times for each male ($n=12$ for $Grn^{+/+}$, $n=10$ for $Grn^{+/-}$, $n=14$ for $Grn^{-/-}$). (A) Latency (left) and frequency (right) of mount. Each symbol and vertical bar represents the mean and S.E.M., respectively. (B) Latency (left) and frequency (right) of intromission. Each symbol and vertical bar represents the mean and S.E.M., respectively. (C) Percentage of mice showing ejaculation in each trial (left) and over the three trials (right). The incidence of ejaculation was determined by the presence of vaginal plugs in females after the test. $^{*}p<0.05$, Fisher's exact probability test, compared to $Grn^{+/+}$, $Grn^{+/-}$ (left) and to $Grn^{+/+}$ (right). (D) Total aggressive bouts toward stimulant females over the three trials. Each column and vertical bar represents the mean and S.E.M., respectively. (E) Serum testosterone concentrations in adult male mice. Each column and vertical bar represents the mean and S.E.M., respectively ($n=4$ for each experimental group).

following EcoRI digestion of genomic DNA. An 8 kb fragment band corresponding to the sequence from exon 5 to exon 13 of the PGRN gene was detected in $Grn^{+/+}$ mice, a 4.3 kb fragment corresponding to PGK-Neo-bpA and endogenous genomic sequences in $Grn^{-/-}$ mice and both 8 and 4.3 kb bands in $Grn^{+/-}$ mice. To further examine the expression of PGRN mRNA, RT-PCR was performed. The 212 bp expected bands were detected in the epididymis, testis, lung and liver when cDNA from $Grn^{+/+}$ mice was used as the template (Fig. 1D). Weak signals were also detected in the brain and kidney of $Grn^{+/+}$ mice. However, no bands were detected in any examined tissues obtained from $Grn^{-/-}$ mice. A 516 bp band corresponding to β-actin was amplified in all tissues examined from both the $Grn^{+/+}$ and $Grn^{-/-}$ mice.

The genotypes of 442 offspring obtained by matings between $Grn^{+/-}$ male and female mice were 28.1% (124/442) $Grn^{+/+}$, 49.3% (218/442) $Grn^{+/-}$ and 22.6% (100/442) $Grn^{-/-}$, which matched with Mendel's laws of inheritance. The mean litter size from $Grn^{-/-}$ pairs was 6.3 ± 0.3 (mean ± S.E.M., $n = 10$), which was not significantly different from that of $Grn^{+/+}$ pairs (7.9 ± 0.2, $n = 18$). The mean number of weaned pups at 30 days of age was also not significantly different between $Grn^{+/+}$ parents (6.9 ± 0.2, $n = 15$) and $Grn^{-/-}$ parents (4.7 ± 0.3, $n = 9$).

3.2. Male sexual behaviour

The data regarding male sexual behaviour are shown in Fig. 2. The latency and frequency of mount and intromission were not significantly different among the three genotypes throughout the three trials (Fig. 2A and B). However, ejaculation incidence was lower in $Grn^{-/-}$ mice compared to $Grn^{+/+}$ and $Grn^{+/-}$ mice throughout the trials and was significantly different at the second trial (Fig. 2C, left). The percentage of mice displaying ejaculation at least once over the three trials was also significantly lower in $Grn^{-/-}$ mice than that in $Grn^{+/+}$ mice (Fig. 2C, right). Since aggressive behaviours toward females were observed dur-

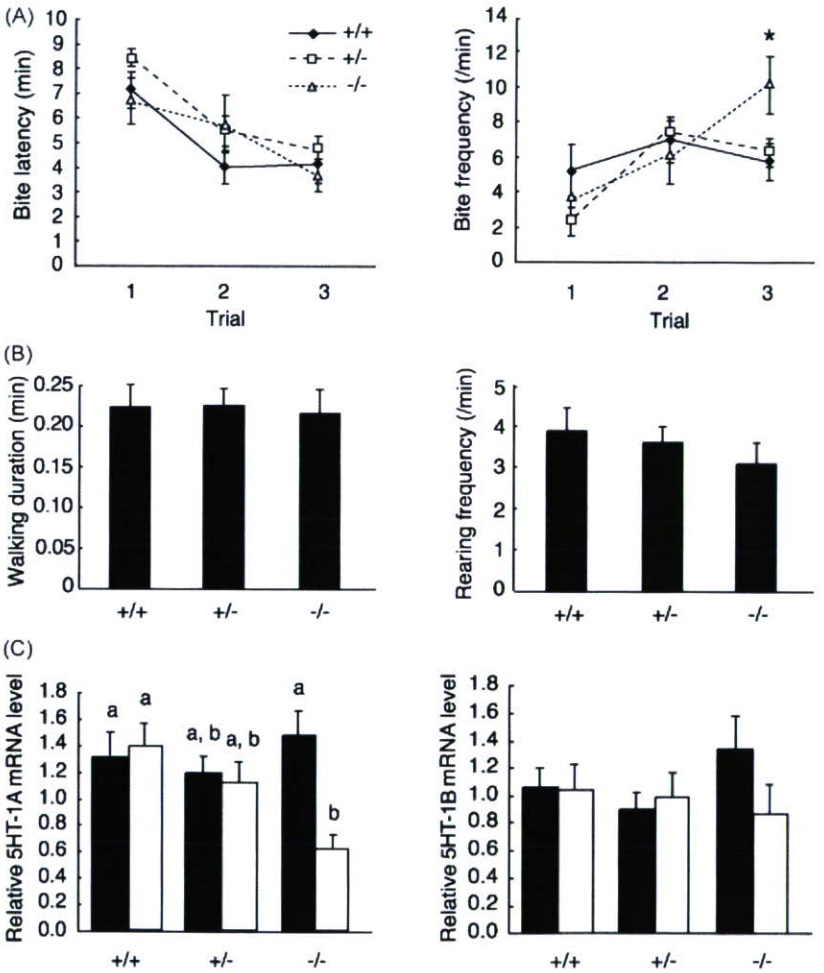

Fig. 3. Analysis of aggressive behaviour. The resident–intruder paradigm was used to assess inter-male aggression. Each male was tested against a male A/J intruder for 5–15 min and behaviour recorded. Tests were repeated three times for each male ($n = 14$ for $Grn^{+/+}$, $n = 23$ for $Grn^{+/-}$, $n = 12$ for $Grn^{-/-}$). (A) Latency (left) and frequency (right) of biting attack. Each symbol and vertical bar represents the mean and S.E.M., respectively. $^{*}p < 0.05$, two-way ANOVA followed by Fisher's PLSD test, compared to $Grn^{+/+}$, $Grn^{+/-}$. (B) Duration of walking (left) and frequency of rearing (right) during 5 min of the first aggressive behaviour test. Each column and vertical bar represents the mean and S.E.M., respectively. (C) Expression of 5-HT1A (left) and 1B (right) mRNA in the hippocampus. Relative mRNA levels of 5-HT1A and 1B to HPRT in the hippocampus of mice with (open column) or without aggressive encounters (closed column) were determined by real-time PCR. Each column and vertical bar represents the mean and S.E.M., respectively ($n = 9$ for each experimental group). The values with different letters are significantly different ($p < 0.05$, two-way ANOVA followed by Fisher's PLSD test).

ing the sexual behaviour tests, the number of aggressive bouts was also counted in this experiment. Although the total number of aggressive bouts over the three trials was not statistically different among the three genotypes, the number was much larger in $Grn^{-/-}$ than $Grn^{+/+}$ mice, while that of $Grn^{+/-}$ mice was intermediate between the two (Fig. 2D). There was no significant difference in serum testosterone concentrations in males among the three genotypes (Fig. 2E).

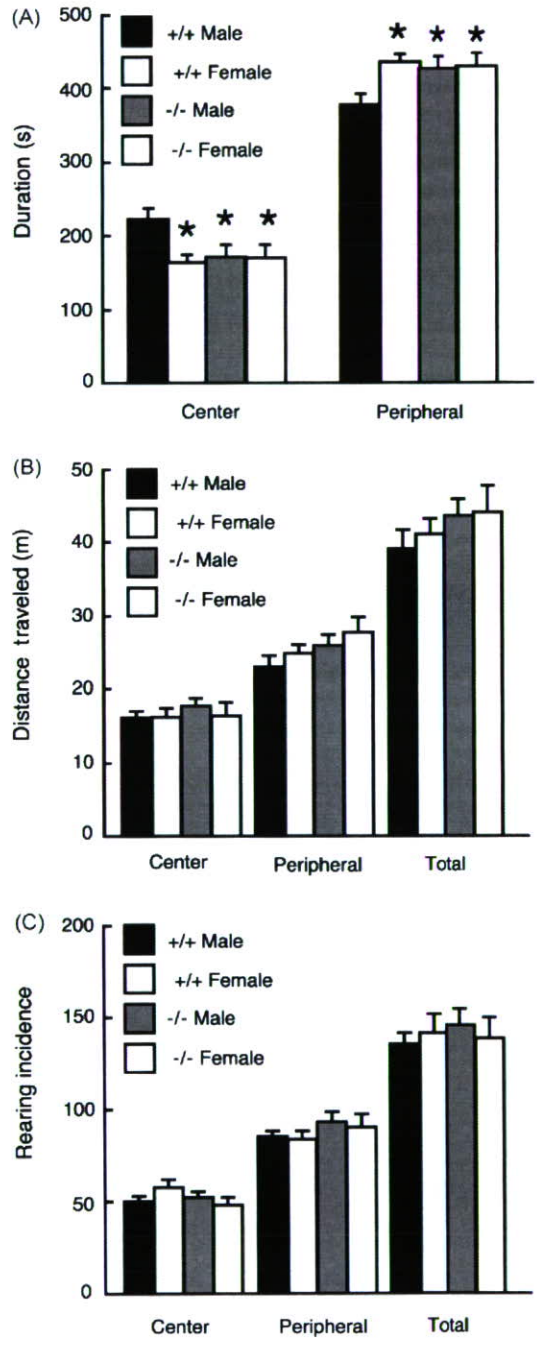

Fig. 4. Analysis of anxiety. Each mouse was placed in the center of the square (open field) and its behaviour was recorded for 10 min. (A) Duration in center, (B) distance traveled and (C) incidence of rearings of male and female $Grn^{+/+}$ and $Grn^{-/-}$ mice. Each column and vertical bar represents the mean and S.E.M., respectively ($n = 13$ for $Grn^{+/+}$ male, $n = 22$ for $Grn^{+/+}$ female, $n = 22$ for $Grn^{-/-}$ male and $n = 14$ for $Grn^{-/-}$ female). $^{*}p < 0.05$, ANOVA followed by Student's t-test, compared to $Grn^{+/+}$ male.

3.3. Aggression

Since $Grn^{-/-}$ mice exhibited prominent, although not significant, aggressive behaviour towards females during the male sexual behaviour test as mentioned above, we evaluated the rate of offensive inter-male fighting by means of a resident–intruder paradigm. As shown in Fig. 3A (left), the latency to the first biting attack tended to be shorter with each trial, although there was no significant difference among the three genotypes. However, as shown in Fig. 3A (right), the frequency of biting attacks in $Grn^{-/-}$ mice was significantly higher than that of $Grn^{+/+}$ and $Grn^{+/-}$ mice at the third trial, although the frequency did not differ among the genotypes in the first and second trials. The duration of walking and the number of rearings, which were recorded during the first trial to evaluate locomotor activity, were not significantly different between the genotypes (Fig. 3B). Since PGRN-deficient mice exhibited enhanced aggressiveness after repeated encounters with intruders, we evaluated the mRNA expression of the serotonergic receptors 5-HT1A and 1B in the hippocampus, which could be related to inhibition of aggression and anxiety, after three instances of aggressive encounters. As shown in Fig. 3C (left), the mRNA expression of 5-HT1A was significantly decreased in the hippocampus of $Grn^{-/-}$ mice that experienced aggressive encounters, while that in $Grn^{+/+}$ and $Grn^{+/-}$ mice remained unchanged. The expression of 5-HT1B mRNA also tended to be decreased following aggressive encounters in $Grn^{-/-}$ mice, but the difference was not significant (Fig. 3C, right). There was no significant difference in both 5-HT1A and 1B mRNA levels among genotypes of mice that did not encounter intruders.

3.4. Anxiety

The levels of anxiety in PGRN-deficient mice were evaluated using the open field test. As shown Fig. 4A, female $Grn^{+/+}$ mice spent significantly less time in the center of the square compared to male $Grn^{+/+}$ mice, although sex difference in the duration staying in the center was not observed in $Grn^{-/-}$ mice. In addition, male $Grn^{-/-}$ mice male spent significantly less time in the center compared to male $Grn^{+/+}$ mice. The distances traveled (Fig. 4B) and incidence of rearing (Fig. 4C) in the center, peripheral zone and the total were not different between sex nor genotypes.

4. Discussion

In the present study, we generated mice with targeted disruption of the PGRN gene to investigate the possible role of PGRN/granulins in the brain. Since it is reported that PGRN is expressed in the acrosome of the sperm [3] and oocytes [47] and that PGRN modulates the development of early embryos *in vitro* [19], we suspected that $Grn^{-/-}$ mice might be fetal lethal or exhibit disorders in reproductive function. However, they were fertile, and both litter size and the number of weaned pups were not different between $Grn^{+/+}$ pairs and $Grn^{-/-}$ pairs. It is therefore suggested that PGRN is not necessarily a critical factor

for fertilization and development, especially *in vivo*, in which numerous factors are likely to be involved.

4.1. Attenuation of sexual behaviour

In the male sexual behaviour analysis, the latency and frequency of mount and intromission were not significantly different among the three genotypes, yet ejaculation incidence and the number of mice displaying ejaculation were significantly lower in $Grn^{-/-}$ mice compared to $Grn^{+/+}$ and $Grn^{+/-}$ males. We have previously shown that neonatal treatment of the male rat brain with antisense oligodeoxynucleotides for the PGRN gene suppressed all mount, intromission and ejaculation [46]. The precise reason for this discrepancy is unknown; however, the processes of brain sexual differentiation may vary between rats and mice. The dogma that estrogens converted from androgens masculinize the neonatal brain is mostly derived from the results from rat experiments, but this may not be the case for mice. This fact has come to light recently with the generation of many kinds of knockout (KO) mice in the research fields of reproduction and neuroscience. For example, data from aromatase KO [5] and estrogen receptor (ER) KO [53] male mice suggest that the lack of exposure to, or receptors for, estrogens during development impairs, but does not necessarily eliminate, expression of male sexual behaviour in adulthood. This may be one of the reasons why complete suppression of male sexual behaviour was not seen in the $Grn^{-/-}$ mice.

The mechanisms for inducing ejaculation are known to differ from those of mount and intromission. Although the medial preoptic area and medial amygdala are regarded as the main controlling sites of male sexual behaviour [36], ejaculation is also mediated by the spinal control center [15]. In addition, the form of the steroid that activates the behaviour seems different [37]. When 5α-dihydrotestosterone (DHT) or 17β-estradiol (E_2) was administered to castrated male mice, E_2 restored mount and intromission to the same extent as DHT, but ejaculation was not restored to the same extent by E_2 compared to DHT. Furthermore, even in castrated male androgen receptor (AR) KO mice, E_2 restored mount and intromission to some extent, but not ejaculation [40]. These observations suggest that mount and intromission can be activated by estrogens as well as androgens, but that ejaculation is activated through AR-mediated processes. In $Grn^{-/-}$ mice, the neuronal structure(s) inducing ejaculation in response to androgens may not be normally differentiated. Since serum testosterone levels were not different among genotypes, PGRN does not seem to affect the neuroendocrine system controlling gonadotropin secretion.

4.2. Augmentation of aggression and anxiety

During the male sexual behaviour test, aggressive behaviour toward females was noticed in $Grn^{-/-}$ mice. Moreover, the total number of aggressive bouts over the three trials tended to be higher in $Grn^{-/-}$ than in $Grn^{+/+}$ or $Grn^{+/-}$ mice. We therefore further investigated inter-male aggression by means of the resident–intruder paradigm. Although bite latency was not different among the three genotypes in any of the trials, the frequency of biting attacks was significantly higher at the third trial in $Grn^{-/-}$ mice compared with $Grn^{+/+}$ and $Grn^{+/-}$ littermates. These changes in aggressive behaviour were well correlated with changes in mRNA expression of serotonergic receptors in the hippocampus, which were involved in reducing aggression and anxiety [18,51]. We observed that it took longer for $Grn^{-/-}$ mice to stop attacking once they started regardless of the intruder's submission, which could be regarded as "impulsive" aggression.

Territorial aggression, as assessed by the resident–intruder paradigm, is regarded as one of the male-dominant behaviours [37], and therefore, the present results can be interpreted such that the brain of male $Grn^{-/-}$ mice could be "hypermasculinized". This conflicts with our above-mentioned notion that PGRN/granulins mediate the masculinizing effects of sex steroids on the brain. While it is difficult to reconcile this discrepancy, we consider the increased aggression in $Grn^{-/-}$ mice to be related to an increase in anxiety rather than male-type sex role behaviour. This is because $Grn^{-/-}$ mice showed aggressive behaviours toward not only males, but also females, and they displayed a significant increase in the level of anxiety in the open field test. In addition, elevated anxiety is often associated with an increase in aggression [26]. It is of interest that females displayed higher levels of anxiety than males in our open field experimental paradigm. Taken together, it is probable that the enhancement of aggression in male PGRN-deficient mice is derived from elevated anxiety due to insufficient masculinization of the brain. Alternatively, female-directed aggression during mating test as well as increased aggression only after repeated exposure to an intruder may suggest an impairment in gender and/or social recognition. This would be in agreement with results from the ERα and ERβ KO mice [12], and also support that estrogen actions in the brain are at least partially mediated by PGRN.

4.3. Possible alteration in the serotonergic system

As mentioned above, 5-HT1A mRNA levels were significantly decreased in the hippocampus of PGRN-deficient mice that experienced aggressive encounters. At present, the mechanism underlying this phenomenon is unclear, but since stress is one of the factors inducing aggressive behaviour [31,49] and exposure to acute stress reduces mRNA expression of 5-HT1A in the hippocampus [29], the serotonergic system of PGRN-deficient mice may be more susceptible to stress, e.g., by encounter with unfamiliar situations, including the presence of intruders.

PGRN/granulins may be related to the organization and/or activation of the serotonergic system in the brain. Alterations in serotonergic neurotransmission have been found in many of the KO mice that display unusual aggressive behaviour [10,39,41]. Serotonergic systems are reported to retain their plasticity after birth in the neonatal period [52] or even up to the weaning period [27], and their distribution and density are influenced by internal environmental facilitators, such as nourishment and growth factors. Moreover, the brain serotonergic system is under the influence of sex steroids [13,14,44,55]. Since PGRN functions as a growth factor the expression of which is regulated by sex

steroids [30,48], it is probable that PGRN mediates the effects of sex steroids on the serotonergic system. Since some of the phenotypes displayed by $Grn^{-/-}$ mice are similar to those of βERKO mice, which have longer ejaculation latency [50], higher aggressiveness described as "impulsive" [35], and lower serotonin content in several brain regions [25], PGRN gene expression may be modulated through ERβ rather than ERα.

Recently, PGRN gene mutations were identified as the responsible factor for familial FTD [4,16]. FTD is characterized by progressive changes in behaviour, personality and language with atrophy of the frontal and temporal lobe of the cerebral cortex [34]. Emotional disturbances, such as dysthymia, anxiety and anger or aggressive behaviour have been also reported in FTD patients [33]. These behavioural and emotional changes may result from the deficits of the serotonergic system, since several studies have indicated the efficacy of treatment with selective serotonin-reuptake inhibitors [21,24] and 5-HT receptor agonists [28] for these symptoms. In addition, decreased levels of serotonin receptors in the cerebral cortices of FTD patients have been reported [20,38]. These observations also support the involvement of PGRN/granulins in modulating the brain serotonergic system.

In conclusion, the present study suggests that PGRN is involved in exhibiting some sexual dimorphic behaviour at least partially by modulating the brain serotonergic system. Although further studies are needed to clarify the precise mechanisms underlying changes in behavioural phenotypes in PGRN-deficient mice, PGRN may play multiple roles in the brain including sexual differentiation at the perinatal period, neurogenesis in the adult hippocampus [11] and the onset of FTD at old ages [4,16].

Acknowledgements

Y.K. and S.C. equally contributed to this work. This work was supported by Grants-in-Aid for Scientific Research (17208025, 17052003 to M.N.) from the Japan Society for the Promotion of Science and the Ministry of Education, Culture, Sports, Science and Technology of Japan.

References

[1] Arnold AP, Gorski RA. Gonadal steroid induction of structural sex differences in the central nervous system. Ann Rev Neurosci 1984;7:413–42.
[2] Asano M, Furukawa K, Kido M, Matsumoto S, Umesaki Y, Kochibe N, et al. Growth retardation and early death of β-1,4-galactosyltransferase knockout mice with augmented proliferation and abnormal differentiation of epithelial cells. EMBO J 1997;16:1850–7.
[3] Baba T, Nemoto H, Watanabe K, Arai Y, Gerton GL. Exon/intron organization of the gene encoding the mouse epithelin/granulin precursor (acrogranin). Eur J Biochem 1993;322:89–94.
[4] Baker M, Mackenzie IR, Pickering-Brown SM, Gass J, Rademakers R, Lindholm C, et al. Mutations in progranulin cause tau-negative frontotemporal dementia linked to chromosome 17. Nature 2006;442:916–9.
[5] Bakker J, Honda S, Harada N, Balthazart J. Restoration of male sexual behavior by adult exogenous estrogens in male aromatase knockout mice. Horm Behav 2004;46:1–10.
[6] Bateman A, Belcourt D, Bennett H, Lazure C, Solomon S. Granulins, a novel class of peptides from leukocytes. Biochem Biophys Res Commun 1990;173:1161–8.
[7] Bateman A, Bennett HPJ. Granulins: the structure and function of an emerging family of growth factors. J Endocrinol 1998;158:145–51.
[8] Bhandari V, Palfree RG, Bateman A. Isolation and sequence of the granulin precursor cDNA from human bone marrow reveals tandem cysteine-rich granulin domains. Proc Natl Acad Sci USA 1992;89:1715–9.
[9] Bhandari V, Giaid A, Bateman A. The complementary deoxyribonucleic acid sequence, tissue distribution, and cellular localization of the rat granulin precursor. Endocrinology 1993;133:2682–9.
[10] Cases O, Seif I, Grimsby J, Gaspar P, Chen K, Pournin S, et al. Aggressive behavior and altered amounts of brain serotonin and norepinephrine in mice lacking MAO-A. Science 1995;268:1763–6.
[11] Chiba S, Suzuki M, Yamanouchi K, Nishihara M. Involvement of granulin in estrogen-induced neurogenesis in the adult rat hippocampus. J Reprod Dev 2007;53:297–307.
[12] Choleris E, Gustafsson JA, Korach KS, Muglia LJ, Pfaff DW, Ogawa S. An estrogen-dependent four-gene micronet regulating social recognition: a study with oxytocin and estrogen receptor-α and -β knockout mice. Proc Natl Acad Sci USA 2003;100:6192–7.
[13] Cologer-Clifford A, Simon NG, Richter ML, Smoluk SA, Lu S. Androgens and estrogens modulate 5-HT1A and 5-HT1B agonist effects on aggression. Physiol Behav 1999;65:823–8.
[14] Connell S, Karikari C, Hohmann CF. Sex-specific development of cortical monoamine levels in mouse. Dev Brain Res 2004;151:187–91.
[15] Coolen LM, Allard J, Truitt WA, McKenna KE. Central regulation of ejaculation. Physiol Behav 2004;83:203–15.
[16] Cruts M, Gijselinck I, van der Zee J, Engelborghs S, Wils H, Pirici D, et al. Null mutation in progranulin cause ubiquitin-positive frontotemporal dementia linked to chromosome 17q21. Nature 2006;442:920–4.
[17] Daniel R, He Z, Carmichael KP, Halper J, Bateman A. Cellular localization of gene expression for progranulin. J Histochem Cytochem 2000;48:999–1009.
[18] De Almeida RMM, Rosa MM, Santos DM, Saft DM, Benini Q, Miczek KA. 5-HT1B receptors, ventral orbitofrontal cortex, and aggressive behavior in mice. Psychopharmacology 2006;185:441–50.
[19] Diaz-Cueto L, Stein P, Jacobs A, Schultz RM, Gerton GL. Modulation of mouse preimplantation embryo development by acrogranin (epithelin/granulin precursor). Dev Biol 2000;217:406–18.
[20] Franceschi M, Anchisi D, Pelati O, Zuffi M, Matarrese M, Moresco RM, et al. Glucose metabolism and serotonin receptors in the frontotemporal lobe degeneration. Ann Neurol 2005;57:216–25.
[21] Huey ED, Putnam KT, Grafman J. A systematic review of neurotransmitter deficits and treatments in frontotemporal dementia. Neurology 2006;66:17–22.
[22] Hooper M, Hardy K, Handyside A, Hunter S, Monk M. HPRT-deficient (Lech–Nyhan) mouse embryos derived from germline colonization by cultured cells. Nature 1987;326:292–5.
[23] Horai R, Asano M, Sudo K, Kanuka H, Suzuki M, Nishihara M, et al. Production of mice deficient in genes for interleukin (IL)-1α, IL-1β, IL-1α/β, and IL-1 receptor antagonist shows that IL-1 β is crucial in turpentine-induced fever development and glucocorticoid secretion. J Exp Med 1998;187:1463–75.
[24] Ikeda M, Shigenobu K, Fukuhara R, Hokoishi K, Maki N, Nebu A, et al. Efficacy of fluvoxamine as a treatment for behavioral symptoms in frontotemporal lobar degeneration patients. Dement Geriatr Cogn Disord 2004;17:117–21.
[25] Imwalle D, Gustafsson J, Rissman E. Lack of functional estrogen receptor β influences anxiety behavior and serotonin content in female mice. Physiol Behav 2005;84:157–63.
[26] Kikusui T, Takeuchi Y, Mori Y. Early weaning induces anxiety and aggression in adult mice. Physiol Behav 2004;81:37–42.
[27] Kinney GG, Vogel GW, Feng P. Decreased dorsal raphe nucleus neuronal activity in adult chloral hydrate anesthetized rats following neonatal clomipramine treatment: implications for endogenous depression. Brain Res 1997;756:68–75.
[28] Lebert F, Stekke W, Hasenbroekx C, Pasquier F. Frontotemporal dementia: a randomised, controlled trial with trazodone. Dement Geriatr Cogn Disord 2004;17:355–9.

[29] Lopez JF, Liberzon I, Vazquez DM, Young EA, Watson SJ. Serotonin 1A receptor messenger RNA regulation in the hippocampus after acute stress. Biol Psychiatry 1999;45:934–7.
[30] Lu R, Serrero G. Mediation of estrogen mitogenic effect in human breast cancer MCF-7 cells by PC-cell-derived growth factor (PCDGF/granulin precursor). Proc Natl Acad Sci USA 2001;98:142–7.
[31] Matsumoto K, Pinna G, Puia G, Guidotti A, Costa E. Social isolation stress-induced aggression in mice: a model to study the pharmacology of neurosteroidogenesis. Stress 2005;8:85–93.
[32] McEwen BS, Lieberburg I, Chaptal C, Krey LC. Aromatization: important for sexual differentiation of the neonatal rat brain. Horm Behav 1977;9:249–63.
[33] Mendez MF, McMurtray A, Chen AK, Shapira JS, Mishkin F, Miller BL. Functional neuroimaging and presenting psychiatric features in frontotemporal dementia. J Neurol Neurosurg Psychiatry 2006;77:4–7.
[34] Neary D, Snowden J, Mann D. Frontotemporal dementia. Lancet Neurol 2005;4:771–80.
[35] Ogawa S, Chan J, Chester AE, Gustafsson JA, Korach KS, Pfaff DW. Survival of reproductive behaviors in estrogen receptor β gene-deficient (βERKO) male and female mice. Proc Natl Acad Sci USA 1999;96:12887–92.
[36] Paredes RG, Baum MJ. Role of the medial preoptic area/anterior hypothalamus in the control of masculine sexual behavior. Annu Rev Sex Res 1997;8:68–101.
[37] Pfaff DW. Hormonal processes in the development and expression of aggressive behavior. In: Pfaff DW, editor. Hormones, brain and behavior, vol. 1. New York: Academic Press; 2002. p. 339–92.
[38] Procter AW, Qurne M, Francis PT. Neurochemical features of frontotemporal dementia. Dement Geriatr Cogn Disord 1999;10(Suppl. 1):80–4.
[39] Sallinen J, Haapalinna A, Viitamaa T, Kobilka BK, Scheinin M, Adrenergic. α2c Receptors modulate the acoustic startle reflex, prepulse inhibition and aggression in mice. J Neurosci 1998;18:3035–42.
[40] Sato T, Matsumoto T, Kawano H, Watanabe T, Uematsu Y, Sekine K, et al. Brain masculinization requires androgen receptor function. Proc Natl Acad Sci USA 2004;101:1673–8.
[41] Saudou F, Amara DA, Dierich A, LeMeur M, Ramboz S, Segu L, et al. Enhanced aggressive behavior in mice lacking 5-HT_{1B} receptor. Science 1994;265:1875–8.
[42] Shoyab M, McDonald VL, Byles C, Todaro GJ, Plowman GD. Epithelins 1 and 2: isolation and characterization of two cysteine-rich growth-modulating peptides. Proc Natl Acad Sci USA 1990;87:7912–6.
[43] Soriano P, Montogomery C, Geske R, Bradley A. Targeted disruption of the c-src proto-oncogene leads to osteopetrosis in mice. Cell 1991;64:693–702.
[44] Summer BE, Fink G. Testosterone as well as estrogen increases serotonin 2A receptor mRNA and binding site densities in the male rat brain. Mol Brain Res 1998;59:205–14.
[45] Suzuki M, Yoshida Y, Nishihara M, Takahashi M. Identification of a sex steroid-inducible gene in the neonatal rat hypothalamus. Neurosci Lett 1998;242:127–30.
[46] Suzuki M, Bannai M, Matsumuro M, Furuhata Y, Ikemura R, Kuranaga E, et al. Suppression of copulatory behavior by intracerebroventricular infusion of antisense oligodeoxynucleotide of granulin in neonatal male rats. Physiol Behav 2000;68:707–13.
[47] Suzuki M, Matsumuro M, Hirabayashi K, Ogawara M, Takahashi M, Nishihara M. Oocyte-specific expression of granulin precursor (acrogranin) in rat ovary. J Reprod Dev 2000;46:271–7.
[48] Suzuki M, Yonezawa T, Fujioka H, Matuamuro M, Nishihara M. Induction of granulin precursor gene expression by estrogen treatment in neonatal rat hypothalamus. Neurosci Lett 2001;297:199–202.
[49] Tedeschi RE, Tedeschi DH, Mucha A, Cook L, Mattis PA, Fellows EJ. Effects of various centrally acting drugs on fighting behavior of mice. J Pharmacol Exp Ther 1959;125:28–34.
[50] Temple JL, Scordalakes EM, Bodo C, Gustafsson JA, Rissman EF. Lack of functional estrogen receptor β gene disrupts pubertal male sexual behavior. Horm Behav 2003;44:427–34.
[51] van Riel D, Miijer OC, Veenem AH, Joels M. Hippocampal serotonin responses in short and long attack latency mice. J Neuroendocrinol 2002;14:234–9.
[52] Vitalis T, Cases O, Callebert J, Launay JM, Price DJ, Seif I, et al. Effects of monoamine oxidase A inhibition on barrel formation in the mouse somatosensory cortex: determination of a sensitive developmental period. J Comp Neurol 1998;393:169–84.
[53] Wersinger SR, Sannen K, Villalba C, Lubahn DB, Rissman EF, De Vries GJ. Masculine sexual behavior is disrupted in male and female mice lacking a functional estrogen receptor α gene. Horm Behav 1997;32:176–83.
[54] Yagi T, Nada S, Watanabe N, Tamemoto H, Kohmura N, Ikawa Y, et al. A novel negative selection for homologous recombinants using diphtheria toxin A fragment gene. Anal Biochem 1993;214:77–86.
[55] Zhang L, Ma W, Barker JL, Rubinow DR. Sex difference in expression of serotonin receptors (subtype 1A and 2A) in rat brain: a possible role of testosterone. Neuroscience 1999;94:251–9.

European Journal of Neuroscience, Vol. 26, pp. 2269–2278, 2007 doi:10.1111/j.1460-9568.2007.05829.x

Involvement of protein-tyrosine phosphatase PTPMEG in motor learning and cerebellar long-term depression

Shin-ichiro Kina,[1] Tohru Tezuka,[1] Shinji Kusakawa,[2] Yasushi Kishimoto,[3,4,*] Sho Kakizawa,[5] Koichi Hashimoto,[3,4] Miho Ohsugi,[1] Yuji Kiyama,[2] Reiko Horai,[6] Katsuko Sudo,[6,†] Shigeru Kakuta,[6] Yoichiro Iwakura,[6] Masamitsu Iino,[5] Masanobu Kano,[3,4] Toshiya Manabe[2,7] and Tadashi Yamamoto[1]

[1]Division of Oncology, Department of Cancer Biology, Institute of Medical Science, University of Tokyo, Minato-ku, Tokyo, 108-8639, Japan

[2]Division of Neuronal Network, Department of Basic Medical Sciences, Institute of Medical Science, University of Tokyo, Minato-ku, Tokyo, 108-8639, Japan

[3]Department of Cellular Neurophysiology, Graduate School of Medical Science, Kanazawa University, Kanazawa, 920-8640, Japan

[4]Department of Cellular Neuroscience, Graduate School of Medicine, Osaka University, Suita, 565-0871, Japan

[5]Department of Cellular and Molecular Pharmacology, Graduate School of Medicine, University of Tokyo, Bunkyo-ku, Tokyo, 113-0033, Japan

[6]Division of Cell Biology, Center for Experimental Medicine, Institute of Medical Science, University of Tokyo, Minato-ku, Tokyo, 108-8639, Japan

[7]CREST and RISTEX, Japan Science and Technology Agency

Keywords: cerebellum, eyeblink conditioning, knockout mice, phosphorylation, Purkinje cells

Abstract

Although protein-tyrosine phosphorylation is important for hippocampus-dependent learning, its role in cerebellum-dependent learning remains unclear. We previously found that PTPMEG, a cytoplasmic protein-tyrosine phosphatase expressed in Purkinje cells (PCs), bound to the carboxyl-terminus of the glutamate receptor δ2 via the postsynaptic density-95/discs-large/ZO-1 domain of PTPMEG. In the present study, we generated PTPMEG-knockout (KO) mice, and addressed whether PTPMEG is involved in cerebellar plasticity and cerebellum-dependent learning. The structure of the cerebellum in PTPMEG-KO mice appeared grossly normal. However, we found that PTPMEG-KO mice showed severe impairment in the accelerated rotarod test. These mice also exhibited impairment in rapid acquisition of the cerebellum-dependent delay eyeblink conditioning, in which conditioned stimulus (450-ms tone) and unconditioned stimulus (100-ms periorbital electrical shock) were co-terminated. Moreover, long-term depression at parallel fiber–PC synapses was significantly attenuated in these mice. Developmental elimination of surplus climbing fibers and the physiological properties of excitatory synaptic inputs to PCs appeared normal in PTPMEG-KO mice. These results suggest that tyrosine dephosphorylation events regulated by PTPMEG are important for both motor learning and cerebellar synaptic plasticity.

Introduction

The mammalian cerebellum is important for motor coordination, sensorimotor integration, motor learning and timing to non-motor functions such as cognition (Schmahmann & Sherman, 1998; Ito, 2002; Boyden *et al.*, 2004; Swinny *et al.*, 2005). Motor coordination is a smooth execution of compound movements, whereas motor learning is a process of improving the accuracy and/or efficiency of movements (Ito, 2002; Swinny *et al.*, 2005). Purkinje cells (PCs) provide the sole output from the cerebellar cortex. They receive two distinct excitatory inputs: one from parallel fibers (PFs), the bifurcated axons of granule cells; and the other from climbing fibers (CFs) that originate in the inferior olive. Modulation of PC activity by PF- and CF-inputs contributes to both motor coordination and motor learning.

Correspondence: Dr T. Yamamoto, as above.
E-mail: tyamamot@ims.u-tokyo.ac.jp

**Present address*: Department of Neurobiophysics, Graduate School of Pharmaceutical Sciences at Kagawa campus, Tokushima Bunri University, Sanuki, 769-2193, Japan.

†*Present address*: Animal Research Center, Tokyo Medical University, Tokyo, 160-8402, Japan.

Received 15 January 2007, revised 14 August 2007, accepted 16 August 2007

Cerebellar long-term depression (LTD) at PF–PC synapses is reported to underlie several forms of cerebellum-dependent motor learning, such as classical eyeblink conditioning and adaptation of the vestibulo-ocular reflex (Ito, 2002). In cerebellar LTD, a persistent and input-specific attenuation of the PF–PC synaptic efficacy is induced when PF- and CF-inputs to PC are stimulated together at low frequencies. Cerebellar LTD requires three types of glutamate receptors (GluRs) in PCs, which are metabotropic GluR1 (mGluR1), GluRδ2 and α-amino-3-hydroxy-5-methyl-4-isoxazolepropionic acid type receptors (AMPARs; Ito, 2002). Stimulation of mGluR1 leads to protein kinase C (PKC)-mediated phosphorylation of the AMPAR subunit GluR2. This phosphorylation results in endocytosis of AMPARs and downregulation of AMPAR-mediated synaptic transmission (Chung *et al.*, 2003; Steinberg *et al.*, 2006). GluRδ2 is involved in AMPAR trafficking (Hirai *et al.*, 2003), and several GluRδ2-interacting proteins have been identified (Yuzaki, 2004; Yawata *et al.*, 2006). However, the molecular mechanism by which GluRδ2 participates in cerebellar LTD and motor learning is largely unknown. In addition to serine/threonine phosphorylation, tyrosine phosphorylation events are also implicated in cerebellar LTD and motor learning (Castro-Alamancos & Torres-Aleman, 1994; Boxall

© The Authors (2007). Journal Compilation © Federation of European Neuroscience Societies and Blackwell Publishing Ltd